

Supplementary Materials for
Novel Eye Genes Systematically Discovered through an Integrated Analysis of Mouse Transcriptomes and Phenome

Chia-Yin Chiang, Yung-Hao Ching, Ting-Yan Chang, Liang-Shuan Hu, Yee Siang Yong, Pei Ying Keak, Ivana Mustika, Ming-Der Lin, Ben-Yang Liao

Content

Supplementary Figures

Figure S1. The flowchart to summarize the processes to predict tissue functions of genes in the present study.

Figure S2. Preservation of modules according to Zsummary scores.

Figure S3. Modules in the GNF1M-based coexpression network of mouse genes.

Figure S4. Modules in the MOE430-based coexpression network of mouse genes.

Figure S5. Modules in the RNA-seq-based coexpression network of mouse genes.

Figure S6. Genes associated with the “eye” module, when coexpressed gene modules were defined by PGCNA.

Figure S7. Genes with a higher confidence score of predicted eye functions tend to have a higher Z_{eye} .

Figure S8. Consequences of knocking down the zebrafish ortholog of the mouse gene, *Adal*.

Figure S9. Consequences of knocking down the zebrafish orthologs of the mouse gene, *Ankrd33*.

Figure S10. Consequences of knocking down the zebrafish ortholog of the mouse gene, *Car14*.

Figure S11. Consequences of knocking down the zebrafish ortholog of the mouse gene, *Ccdc126*.

Figure S12. Consequences of knocking down the zebrafish orthologs of the mouse gene, *Dhx32*.

Figure S13. Consequences of knocking down the zebrafish orthologs of the mouse gene, *Dkk3*.

Figure S14. Consequences of knocking down the zebrafish orthologs of the mouse gene, *Fam169a*.

Figure S15. Consequences of knocking down the zebrafish ortholog of the mouse gene, *Frmpd2*.

Figure S16. Consequences of knocking down the zebrafish ortholog of the mouse gene, *Grifin*.

Figure S17. Consequences of knocking down the zebrafish ortholog of the mouse gene, *Kcng14*.

Figure S18. Consequences of knocking down the zebrafish ortholog of the mouse gene, *Irit2*.

Figure S19. Consequences of knocking down the zebrafish orthologs of the mouse gene, *Ppef2*.

Figure S20. Consequences of knocking down the zebrafish orthologs of the mouse gene, *Ppm1n*.

Figure S21. Consequences of knocking down the zebrafish ortholog of the mouse gene, *Tldc1*.

Figure S22. Consequences of knocking down the zebrafish ortholog of the mouse gene, *Wdr17*.

Figure S23. Consequences of knocking down the zebrafish ortholog of the mouse gene, *Pax6d*.

Supplementary Tables

Table S1. The list of tissues whose transcriptomes were profiled by the microarray platform GNF1M and were used to construct the GNF1M-based gene coexpression network.

Table S2. The list of tissues whose transcriptomes were profiled by the microarray platform MOE430 2.0 and were used to construct the MOE430-based gene coexpression network.

Table S3. The list of tissues whose transcriptomes were profiled by the RNA-seq and were used to construct the RNA-seq-based gene coexpression network.

Table S4. The 47 mouse tissues used to functionally annotate gene modules and their corresponding tissue names, presented as MA codes, in MGI for the records of mutant strain phenotyping.

Table S5. Gene modules in the GNF1M-based coexpression network and the associated tissue identified by enrichment analysis based on mutant phenotypes for each module.

Table S6. Gene modules in the MOE430-based coexpression network and the associated tissue identified by enrichment analysis based on mutant phenotypes for each module.

Table S7. Genes modules in the RNA-seq-based coexpression network and the associated tissue identified by enrichment analysis based on mutant phenotypes for each module.

Table S8. The module IDs that were associated with any of the 47 mouse tissues for each of the GNF1M-, MOE430- or RNA-seq-based network.

Table S9. $R_{dcv/phe}$ for each set of genes with a given confidence score and a given predicted tissue function.

Table S10. Enrichment of human orthologs of mouse genes with the top ranked Z_{eye} in genes cataloged in RetNet (dubbed “RetNet”) or HPO-defined eye disease genes (dubbed “HPO”).

Table S11. Mouse genes whose predicted eye functions were supported by all the three datasets (i.e., with a high confidence score).

Table S12. Mouse genes whose predicted eye functions were supported by two of the three datasets (i.e., with a medium confidence score)

Table S13. The number of phenotypically unannotated genes for each set of genes with a given confidence score and a given predicted tissue function.

Table S14. Candidate genes whose vision/eye phenotype have been examined by IMPC, and the gross eye morphology that have been measured in the gene deletion strains.

Table S15. human and zebrafish orthologs of mouse eye candidate genes.

Table S16. Information of morpholino oligoes for functional validation in the zebrafish system.

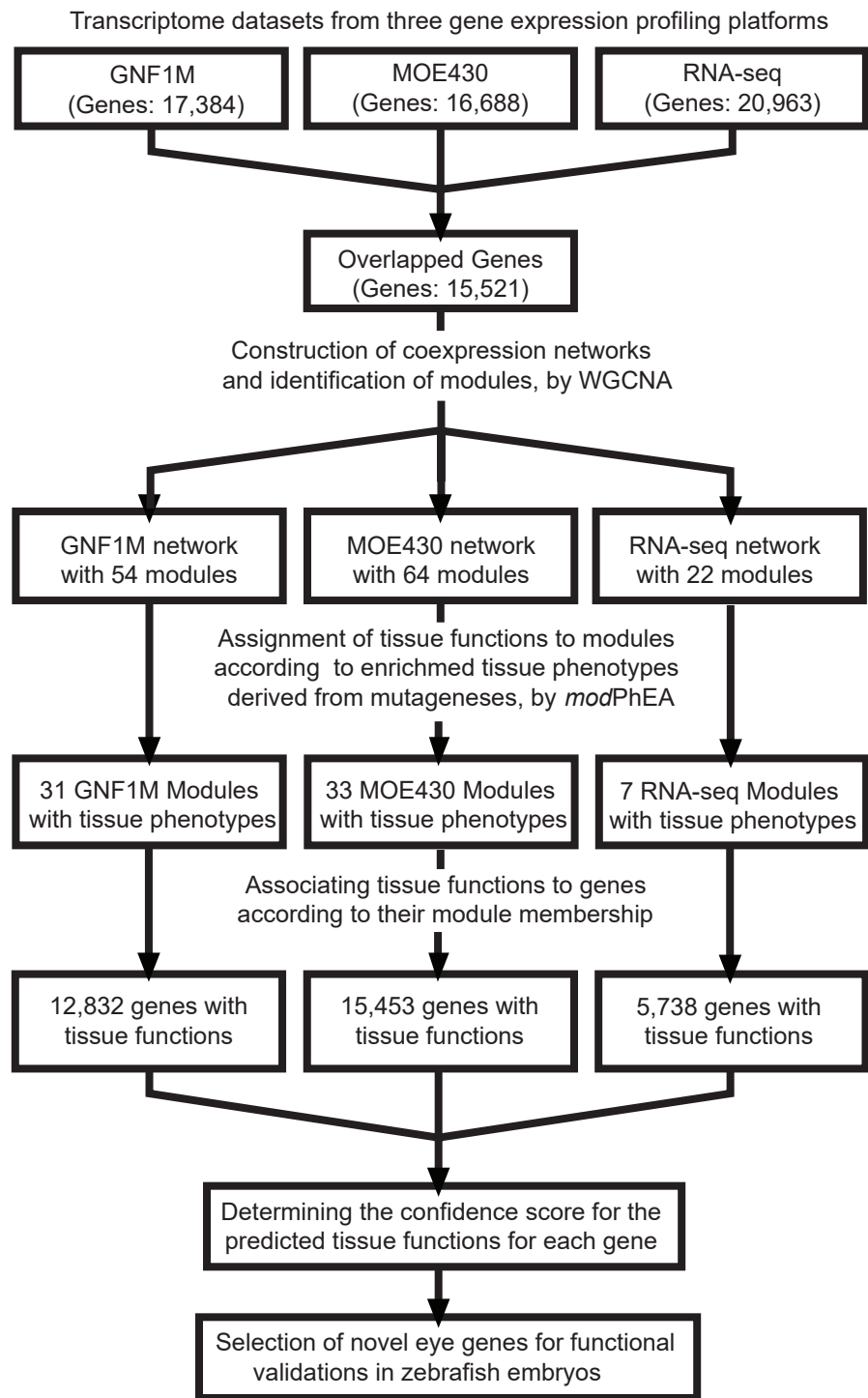


Figure S1. The flowchart to summarize the procedures to predict tissue functions of genes in the present study.

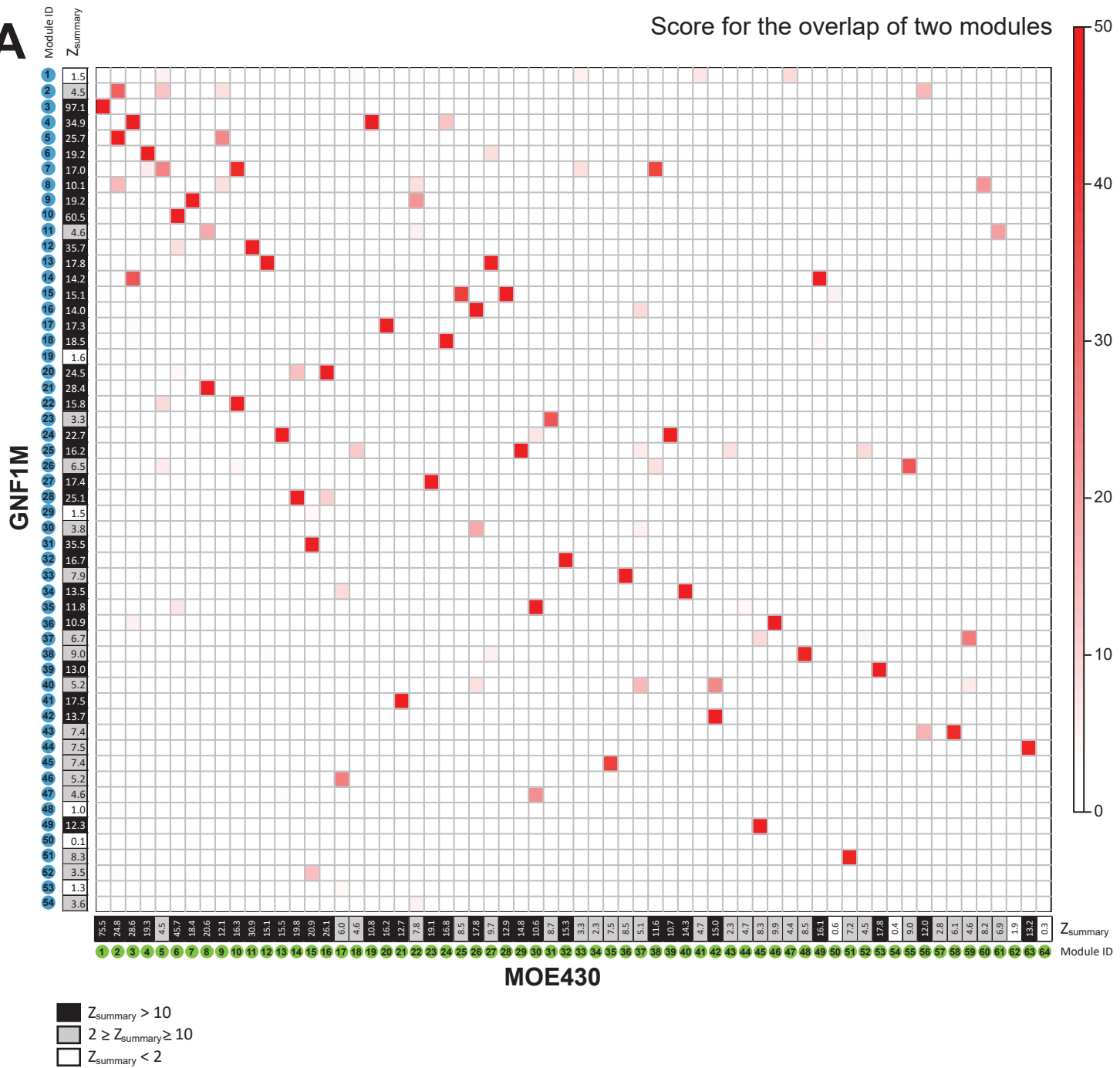
A

Figure S2. Preservation of modules according to Z_{summary} scores. Z_{summary} scores are provided for: (A) GNF1M-based vs. MOE430-based, (B) GNF1M-based vs. RNA-seq-based or (C) MOE430-based vs. RNA-seq-based coexpression genes networks. A $Z_{\text{summary}} > 10$ indicates a high preservation; $10 \geq Z_{\text{summary}} > 2$ indicates a moderate preservation; $Z_{\text{summary}} < 2$ means no preservation. Each score for the overlap of two modules was the -logged P value under the null hypothesis of the number of overlapped genes between the given two modules is expected by chance, according to a Fisher's Exact test. Suppl. Tables S5 – S7 provide descriptions of the module IDs listed in A, B, and C, respectively.

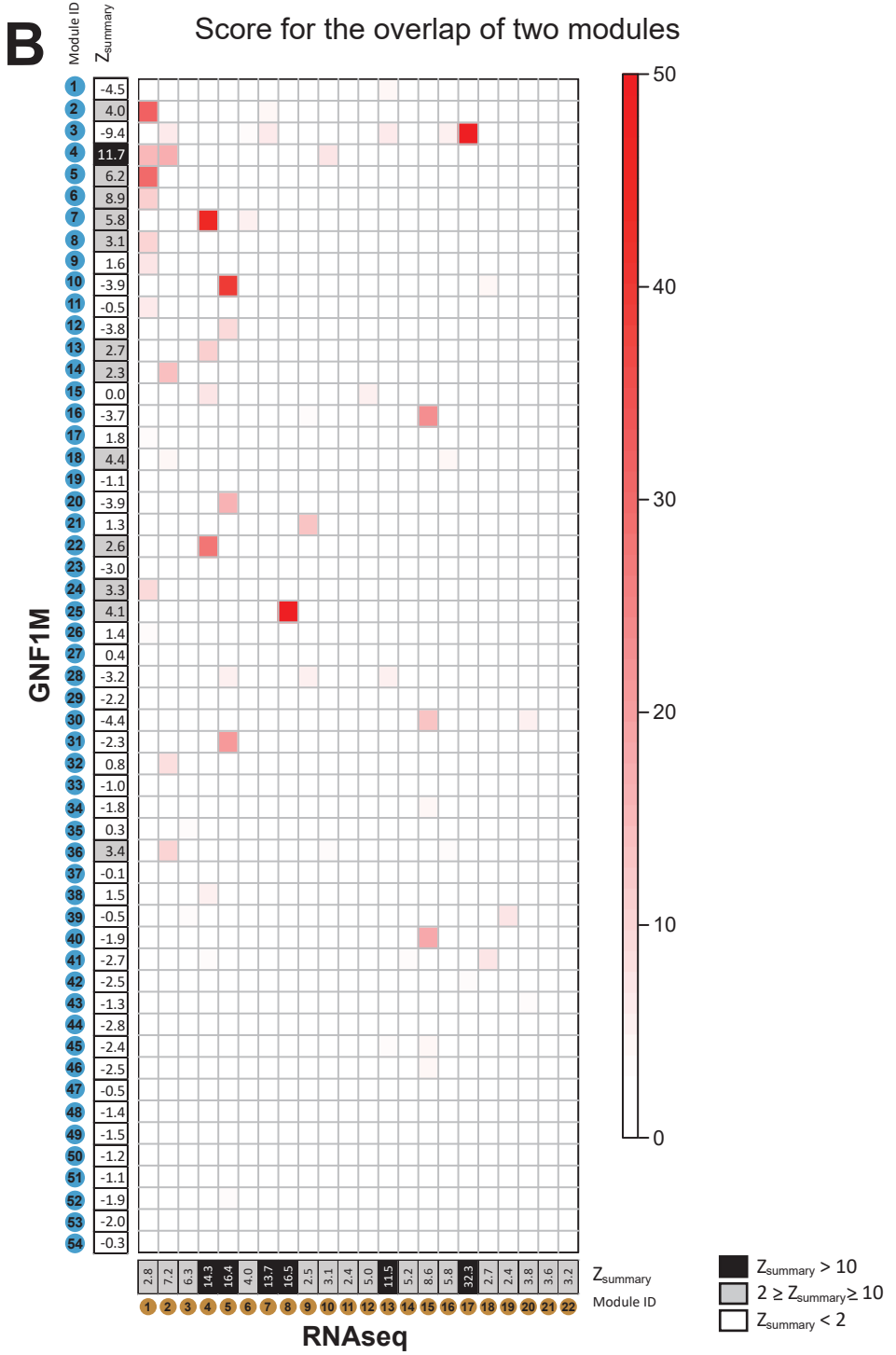


Figure S2. Continued.

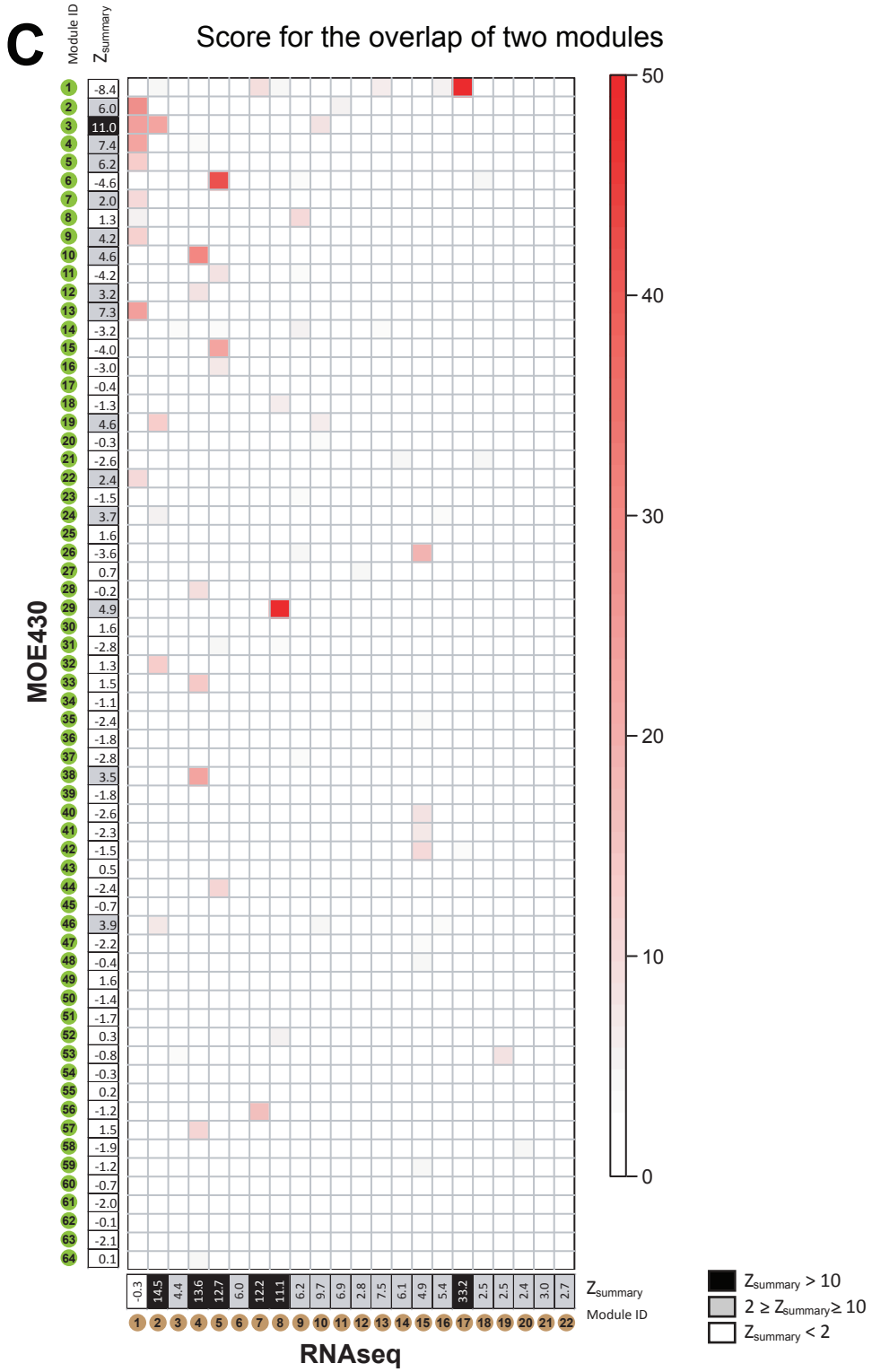


Figure S2. Continued.

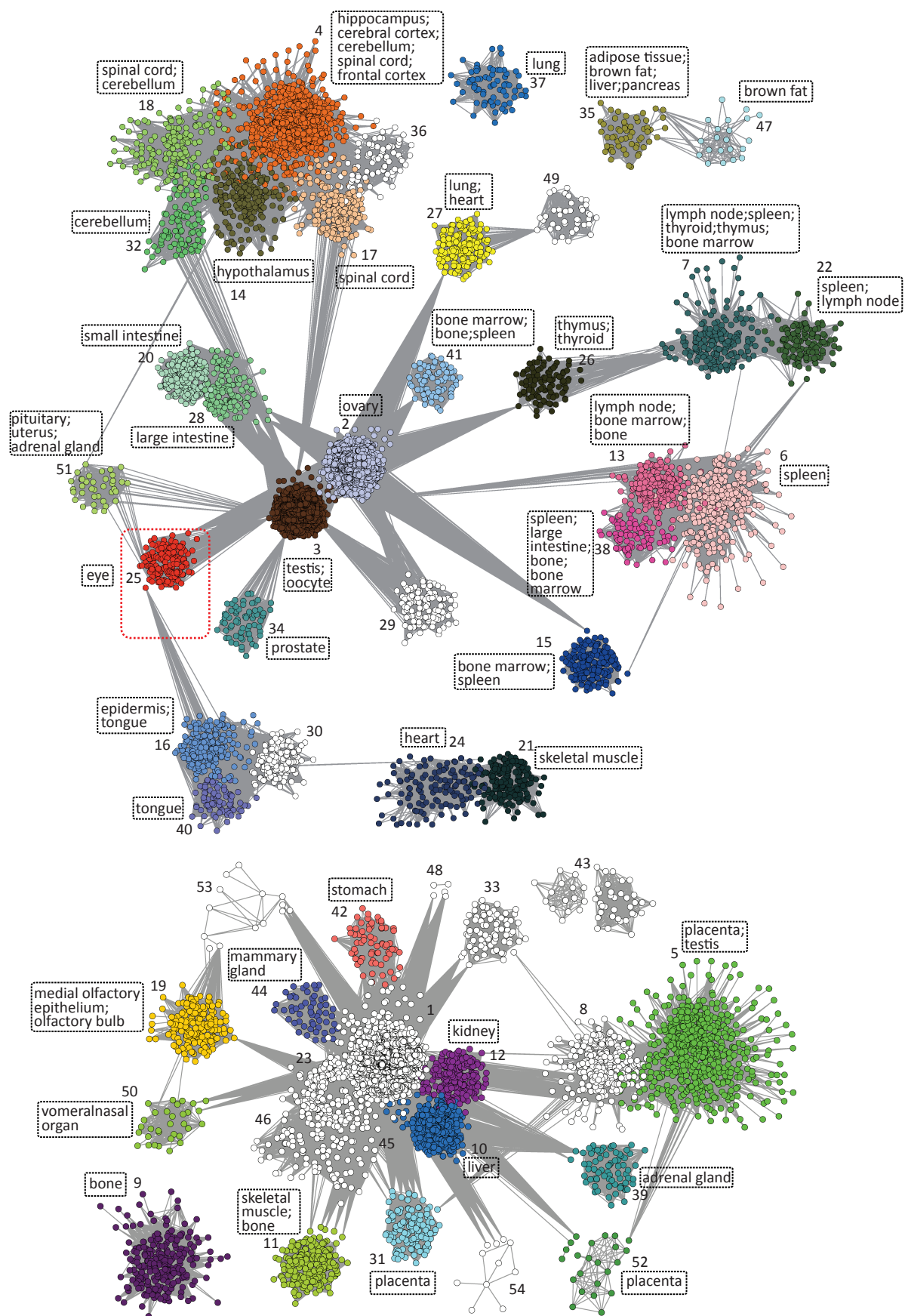


Figure S3. Modules in the GNF1M-based coexpression network of mouse genes. Genes are represented as nodes and each node is connected to all of the other nodes in the weighted network. Only connections with $CoExp \geq 0.3$ are shown for visual convenience. The genes in the modules which could be functionally assigned to at least one of the 42 tissues are colored; while genes in the same module are the same color. The tissue(s) associated with each module are listed in boxes with dashed borders. Module IDs that correspond to Table S5 are indicated for each gene module. Table S5 provides additional statistical details for the 54 modules identified.

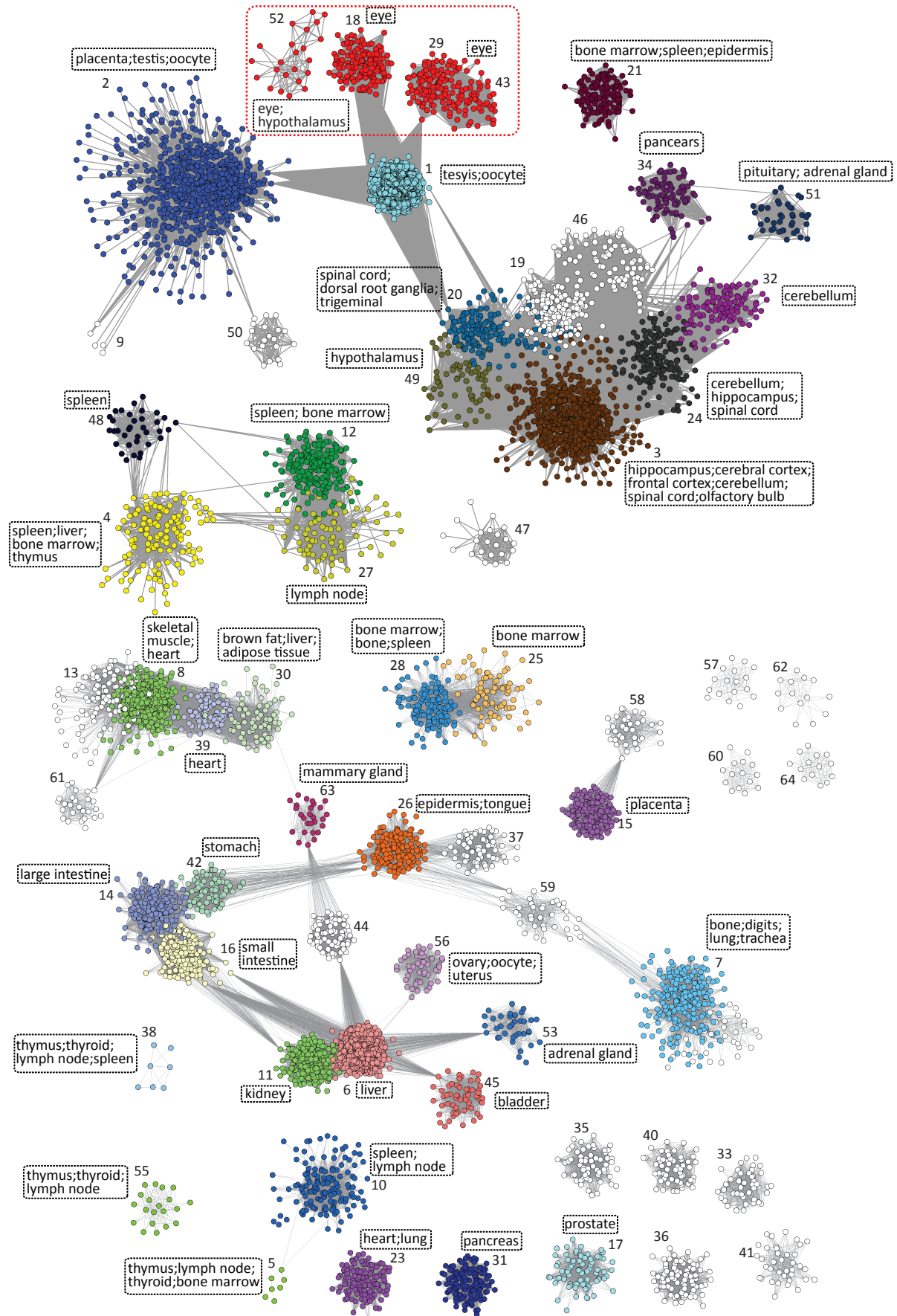


Figure S4. Modules in the MOE430-based coexpression network of mouse genes. Genes are represented as nodes and each node is connected to all of the other nodes in the weighted network. Only connections with $CoExp \geq 0.3$ are shown for visual convenience. The genes in the modules which could be functionally assigned to at least one of the 42 tissues are colored; while genes in the same module are the same color. The tissue(s) associated with each module are listed in boxes with dashed borders. Module IDs that correspond to Table S6 are indicated for each gene module. Table S6 provides additional statistical details for the 64 modules identified.

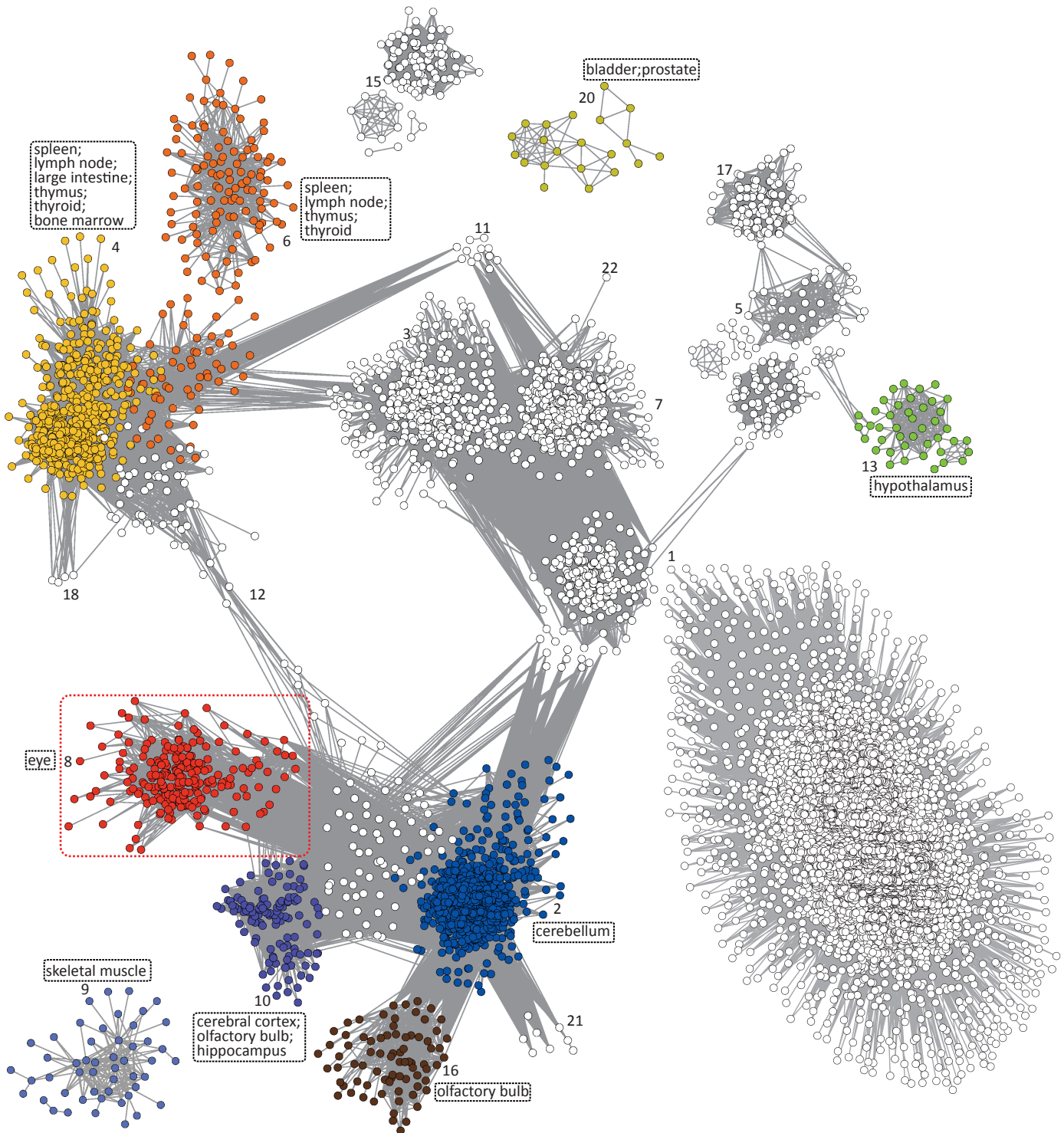


Figure S5. Modules in the RNA-seq-based coexpression network of mouse genes. Genes are represented as nodes and each node is connected to all of the other nodes in the weighted network. Only connections with $CoExp \geq 0.3$ are shown for visual convenience. The genes in the modules which could be functionally assigned to at least one of the 42 tissues are colored; while genes in the same module are the same color. The tissue(s) associated with each module are listed in boxes with dashed borders. Module IDs that correspond to Table S7 are indicated for each gene module. Table S7 provides additional statistical details for the 22 modules identified.

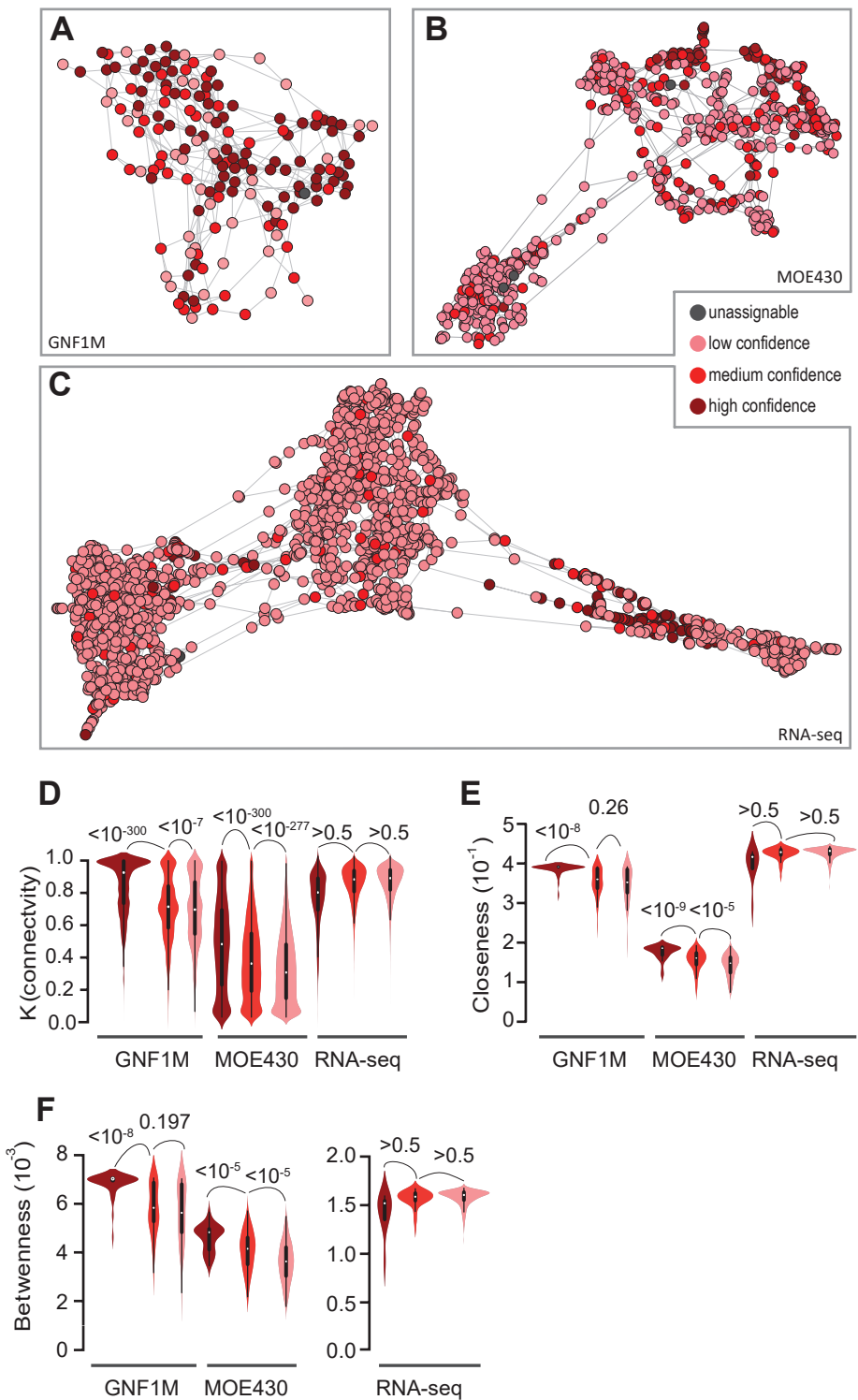


Figure S6 Genes associated with the “eye” module, when coexpressed gene modules were defined by PGCNA. **(A)** Genes with different levels of consistency in being located in the eye module across the three platforms are shown according to their confidence scores [e.g., high (dark red), medium (red), and low (pink)] for predicted retinal function. Only intramodular connections are shown. Genes with higher confidence scores tend to have greater values of **(B)** connectivity, **(C)** betweenness, and **(D)** closeness, thereby indicating that they are more likely to be the central node of the module(s). The corresponding weighted coexpression networks used to generate the data are indicated under each panel. P -values were determined with the Mann-Whitney U -test and are associated with the arched lines that indicate the values that were compared.

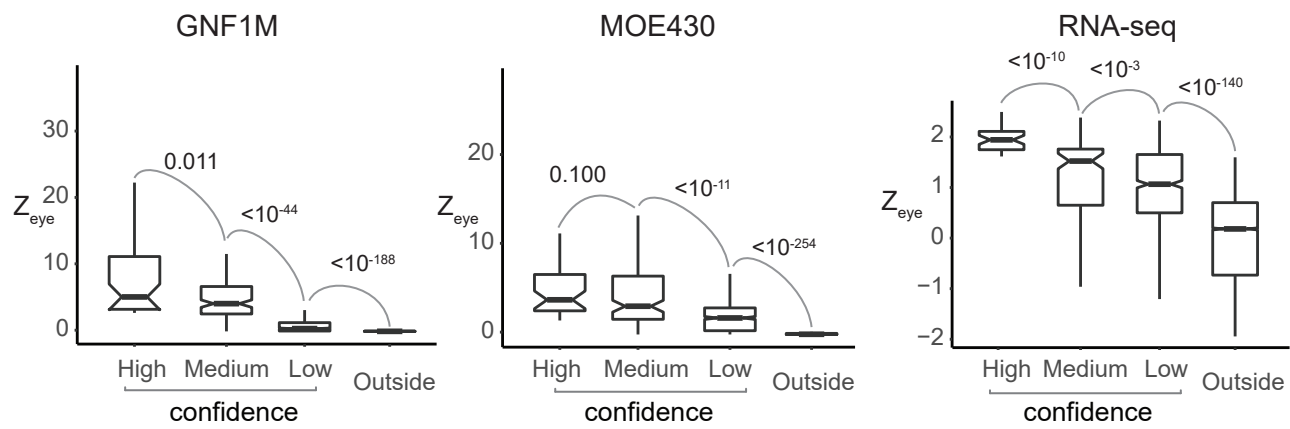


Figure S7. Genes with a higher confidence score of predicted eye functions tend to have a higher Z_{eye} . The boxplots for Z_{eye} values of genes with a “high”, “median” and “low” confidence score and genes outside the eye modules (marked as “outside”) are shown and the adjacent boxes were compared. *P*-values under the null hypothesis of equal median were determined with the Mann-Whitney *U*-test. These values are associated with the arched gray lines connecting the two boxes to indicate the values that were compared.

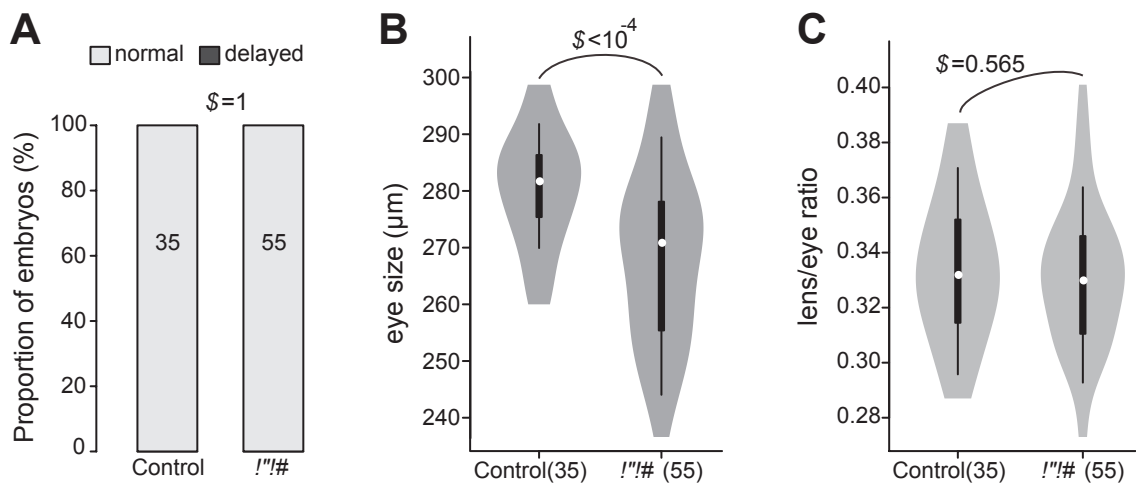


Figure S8. Consequences of knocking down the zebrafish ortholog of the mouse gene, *Adal*, by the group of MO labeled, “*adal*”. The phenotypes measured included: (A) the proportion of normal or delayed embryos, (B) eye size, and (C) lens/eye ratio. *P*-values were determined with (A) Fisher’s exact test or (B, C) the Mann-Whitney *U*-test. These values are associated with the arched gray lines at the top of each panel which indicate the values that were compared. The numbers of samples used to generate the plots are indicated in parentheses.

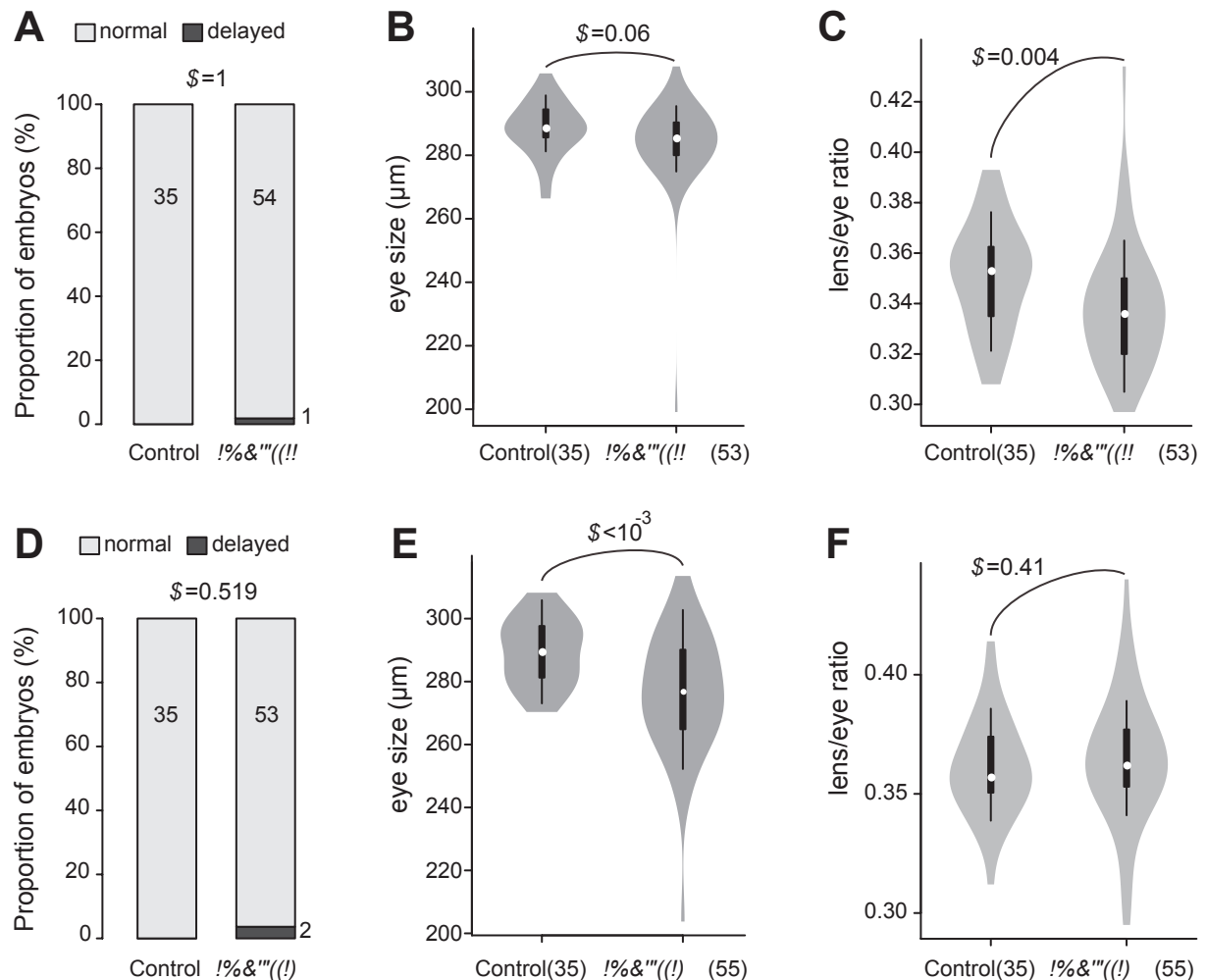


Figure S9. Consequences of knocking down the zebrafish orthologs of the mouse gene, *Ankrd33*, by the groups of MO labeled “*ankrd33aa*” (A-C) and “*ankrd33ab*” (D-F). The phenotypes measured included: (A,D) the proportion of normal or delayed embryos, (B,E) eye size, and (C,F) lens/eye ratio. *P*-values were determined with (A,D) Fisher’s exact test or (B,C,E,F) the Mann-Whitney *U*-test. These values are associated with the arched gray lines at the top of each panel which indicate the values that were compared. The numbers of samples used to generate the plots are indicated in parentheses.

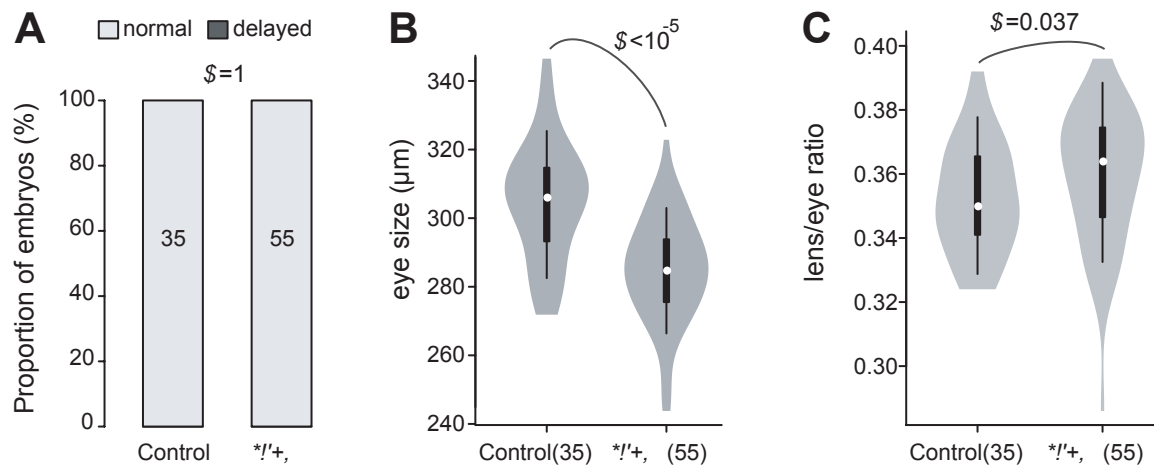


Figure S10. Consequences of knocking down the zebrafish ortholog of the mouse gene, *Car14*, by the group of MO labeled, “*car14*”. The phenotypes measured included: (A) the proportion of normal or delayed embryos, (B) eye size, and (C) lens/eye ratio. *P*-values were determined with (A) Fisher’s exact test or (B, C) the Mann-Whitney *U*-test. These values are associated with the arched gray lines at the top of each panel which indicate the values that were compared. The numbers of samples used to generate the plots are indicated in parentheses.

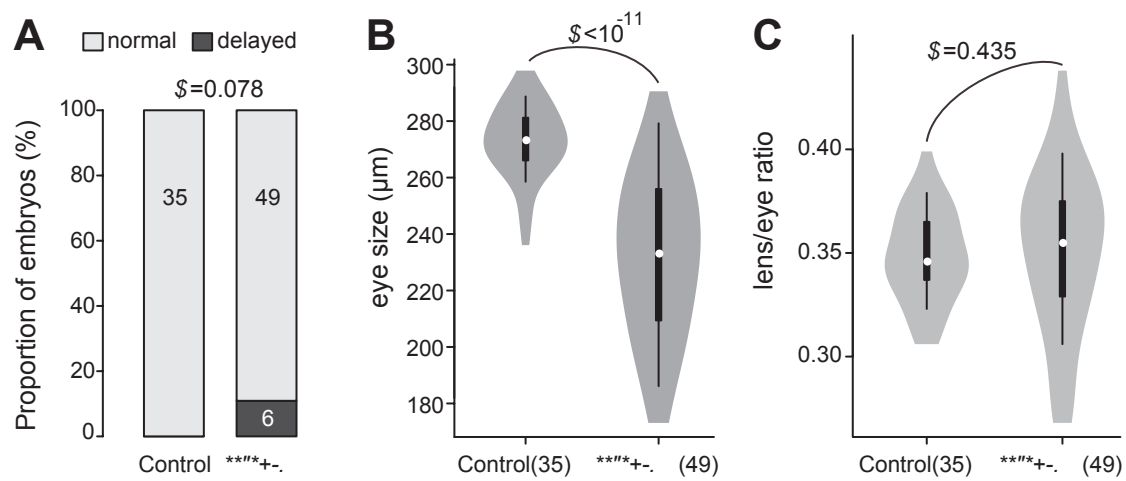


Figure S11. Consequences of knocking down the zebrafish ortholog of the mouse gene, *Ccdc126*, by the group of MO labeled, “*ccdc126*”. The phenotypes measured included: (A) the proportion of normal or delayed embryos, (B) eye size, and (C) lens/eye ratio. *P*-values were determined with (A) Fisher’s exact test or (B, C) the Mann-Whitney *U*-test. These values are associated with the arched gray lines at the top of each panel which indicate the values that were compared. The numbers of samples used to generate the plots are indicated in parentheses.

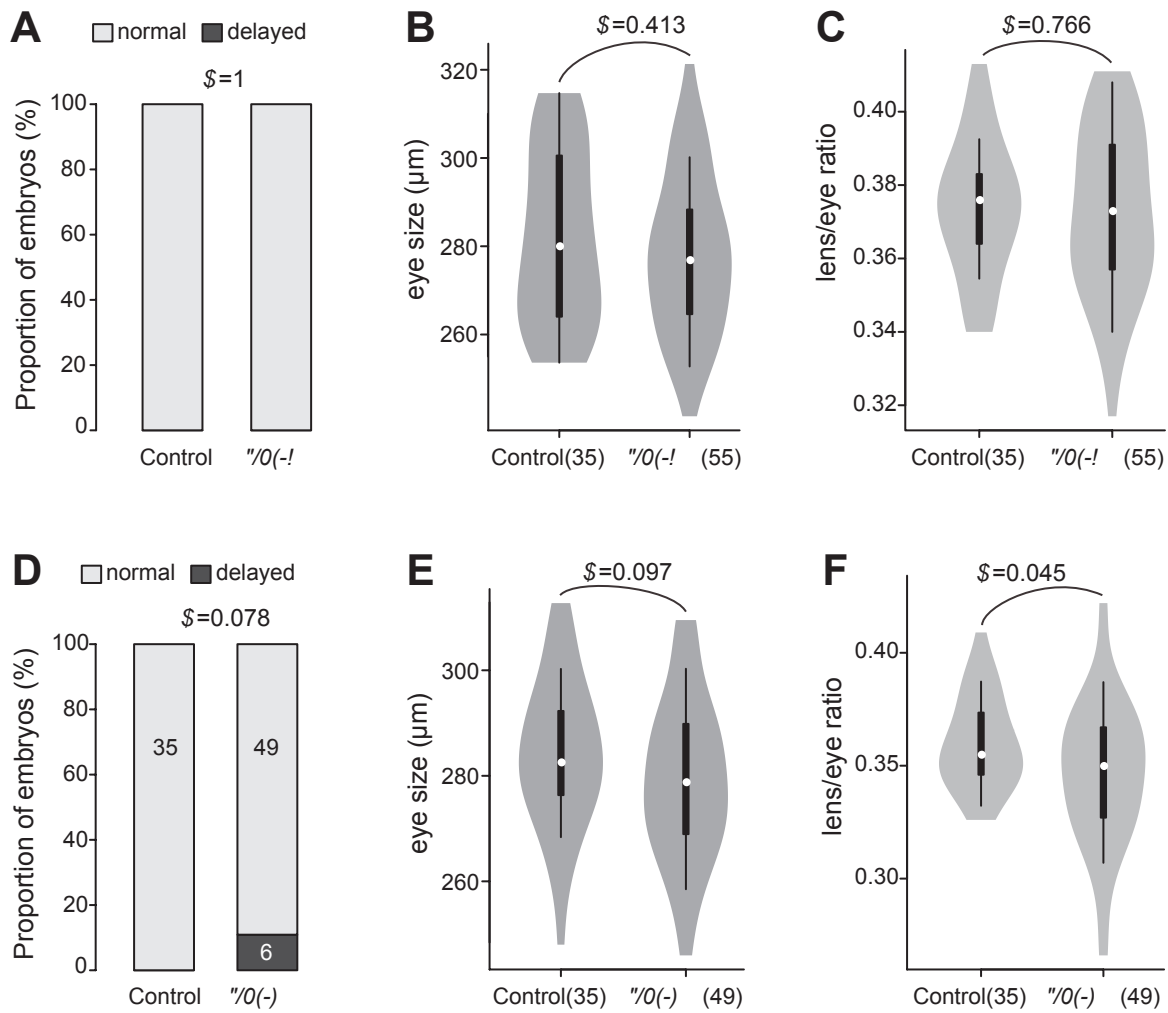


Figure S12. Consequences of knocking down the zebrafish orthologs of the mouse gene, *Dhx32*, by the groups of MO labeled “*dhx32a*” (A-C) and “*dhx32b*” (D-F). The phenotypes measured included: (A,D) the proportion of normal or delayed embryos, (B,E) eye size, and (C,F) lens/eye ratio. *P*-values were determined with (A,D) Fisher’s exact test or (B,C,E,F) the Mann-Whitney *U*-test. These values are associated with the arched gray lines at the top of each panel which indicate the values that were compared. The numbers of samples used to generate the plots are indicated in parentheses.

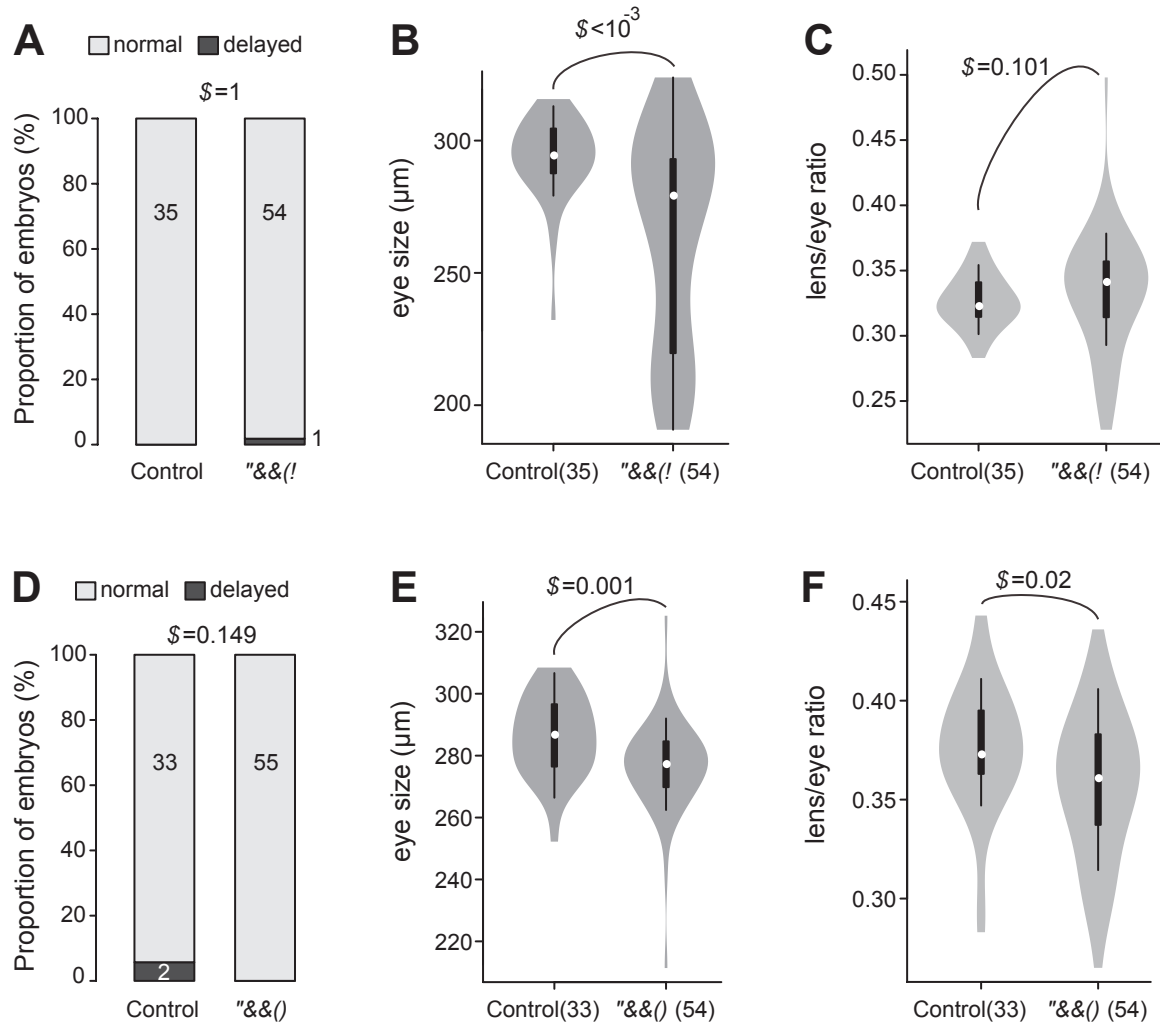


Figure S13. Consequences of knocking down the zebrafish orthologs of the mouse gene, *Dkk3*, by the groups of MO labeled “*dkk3a*” (A-C) and “*dkk3b*” (D-F). The phenotypes measured included: (A,D) the proportion of normal or delayed embryos, (B,E) eye size, and (C,F) lens/eye ratio. *P*-values were determined with (A,D) Fisher’s exact test or (B,C,E,F) the Mann-Whitney *U*-test. These values are associated with the arched gray lines at the top of each panel which indicate the values that were compared. The numbers of samples used to generate the plots are indicated in parentheses.

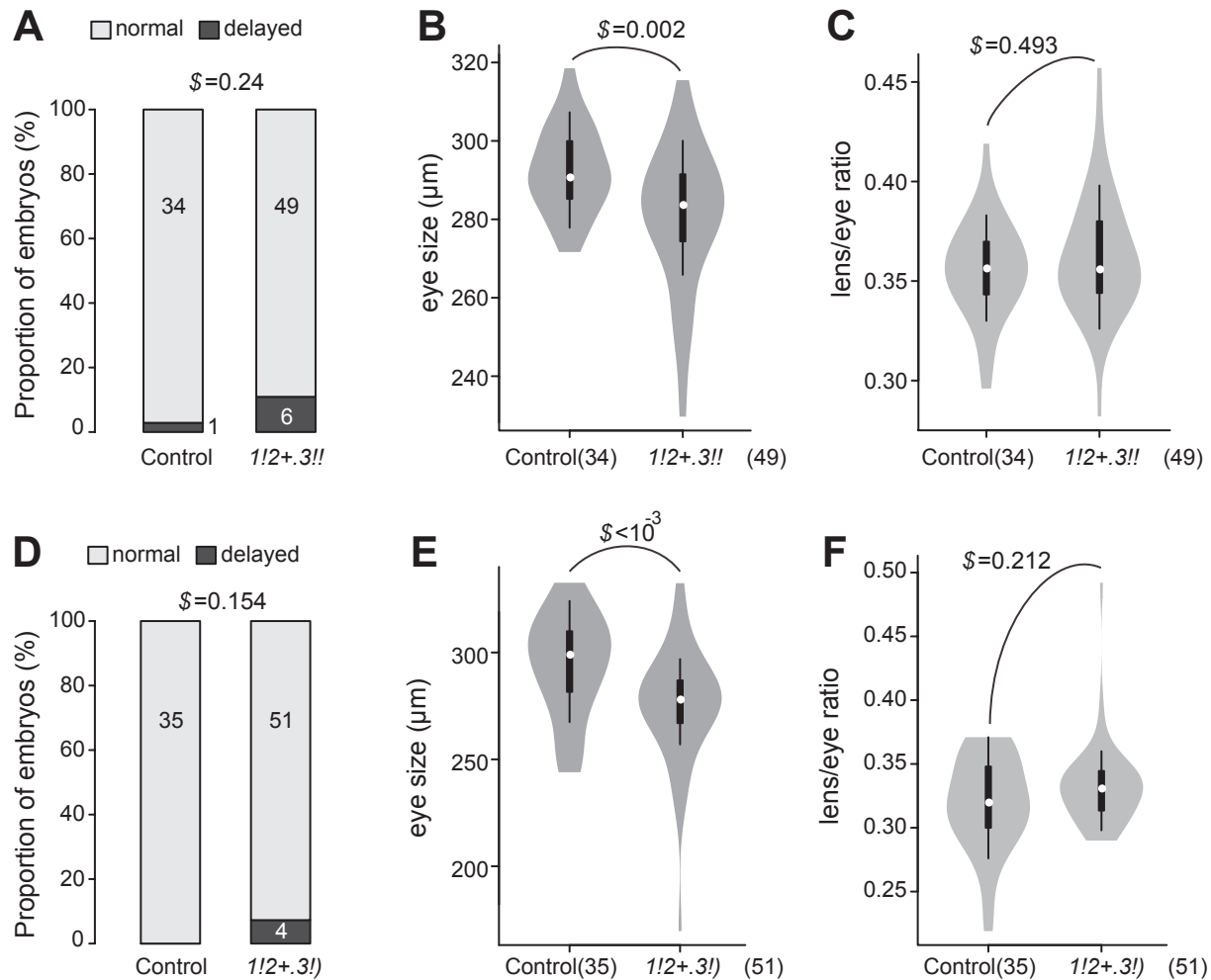


Figure S14. Consequences of knocking down the zebrafish orthologs of the mouse gene, *Fam169a*, by the groups of MO labeled “*fam169aa*” (A-C) and “*fam169ab*” (D-F). The phenotypes measured included: (A,D) the proportion of norlam or delayed embryos, (B,E) eye size, and (C,F) lens/eye ratio. *P*-values were determined with (A,D) Fisher’s exact test or (B,C,E,F) the Mann-Whitney *U*-test. These values are associated with the arched gray lines at the top of each panel which indicate the values that were compared. The numbers of samples used to generate the plots are indicated in parentheses.

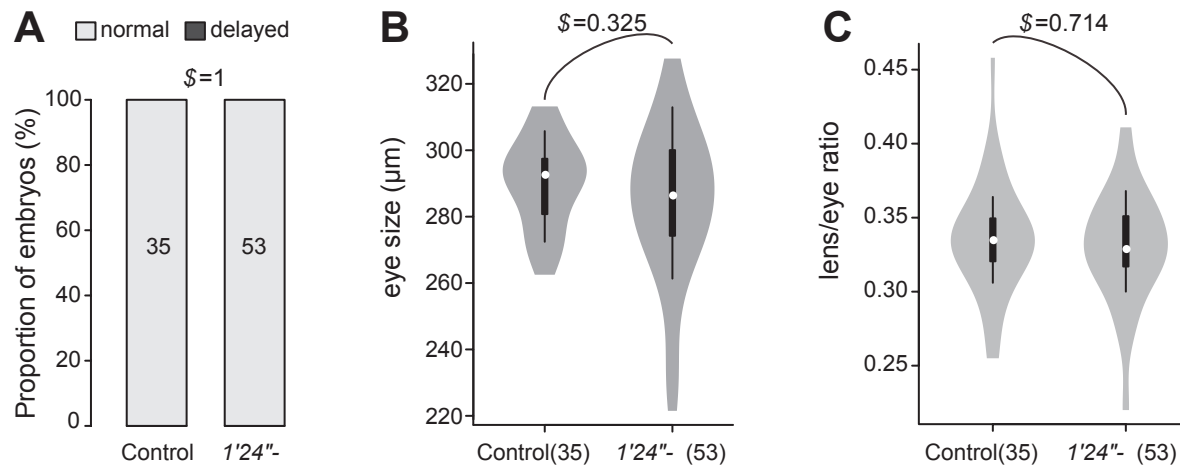


Figure S15. Consequences of knocking down the zebrafish ortholog of the mouse gene, *Frmpd2*, by the group of MO labeled, “*frmpd2*”. The phenotypes measured included: (A) the proportion of normal or delayed embryos, (B) eye size, and (C) lens/eye ratio. *P*-values were determined with (A) Fisher’s exact test or (B, C) the Mann-Whitney *U*-test. These values are associated with the arched gray lines at the top of each panel which indicate the values that were compared. The numbers of samples used to generate the plots are indicated in parentheses.

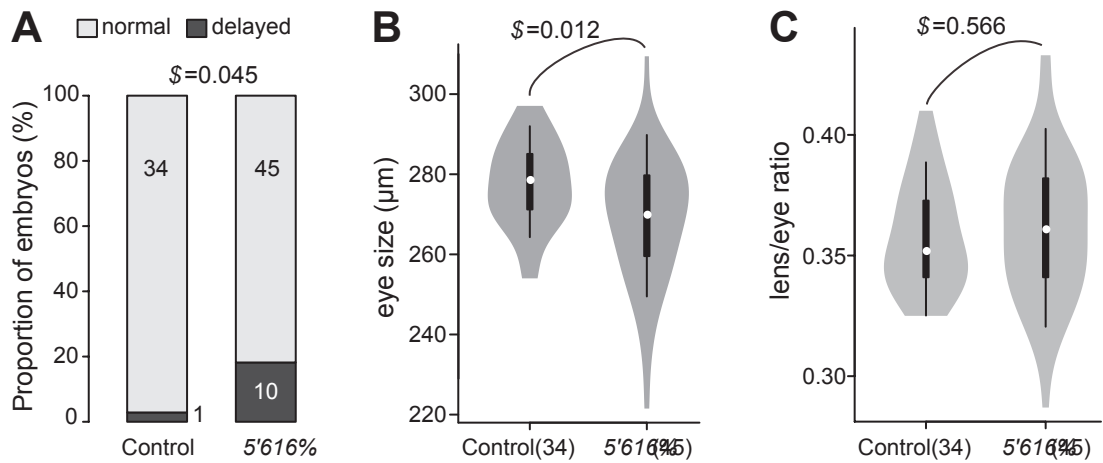


Figure S16. Consequences of knocking down the zebrafish ortholog of the mouse gene, *Grifin*, by the group of MO labeled, “*grifin*”. The phenotypes measured included: **(A)** the proportion of normal or delayed embryos, **(B)** eye size, and **(C)** lens/eye ratio. *P*-values were determined with **(A)** Fisher’s exact test or **(B, C)** the Mann-Whitney *U*-test. These values are associated with the arched gray lines at the top of each panel which indicate the values that were compared. The numbers of samples used to generate the plots are indicated in parentheses.

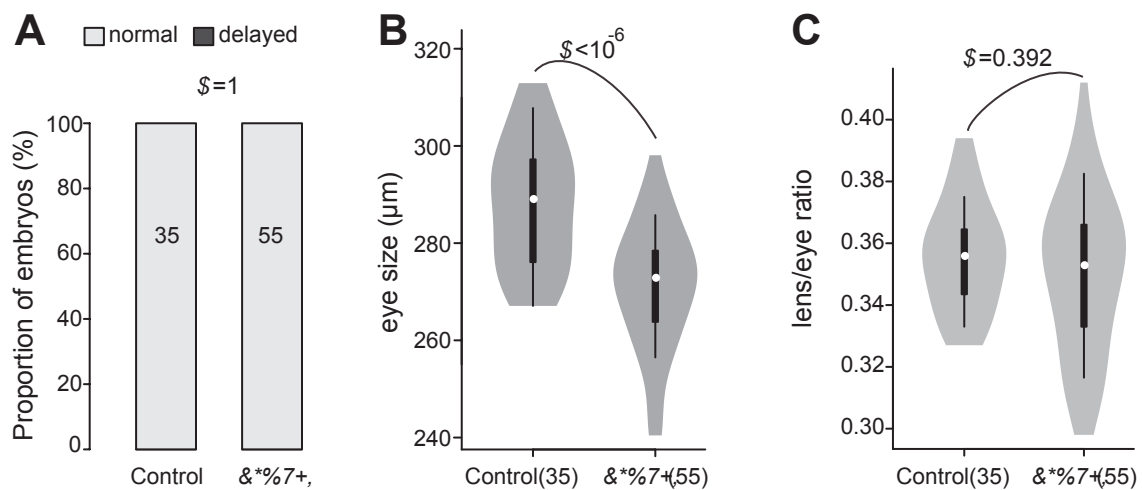


Figure S17. Consequences of knocking down the zebrafish ortholog of the mouse gene, *Kcng14*, by the group of MO labeled, “*kcn14*”. The phenotypes measured included: (A) the proportion of normal or delayed embryos, (B) eye size, and (C) lens/eye ratio. *P*-values were determined with (A) Fisher’s exact test or (B, C) the Mann-Whitney *U*-test. These values are associated with the arched gray lines at the top of each panel which indicate the values that were compared. The numbers of samples used to generate the plots are indicated in parentheses.

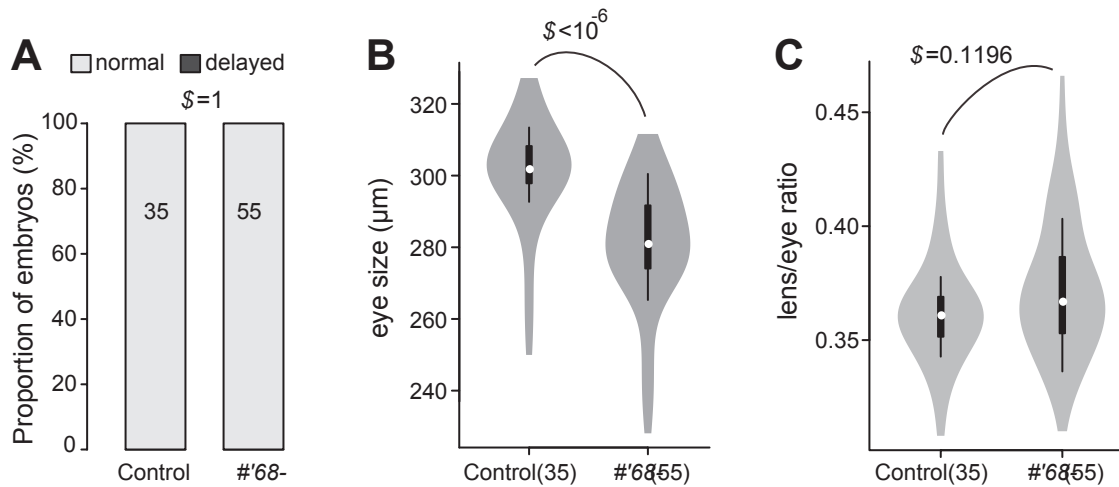


Figure S18. Consequences of knocking down the zebrafish ortholog of the mouse gene, *Lrit2*, by the group of MO labeled, “*lrit2*”. The phenotypes measured included: (A) the proportion of normal or delayed embryos, (B) eye size, and (C) lens/eye ratio. *P*-values were determined with (A) Fisher’s exact test or (B, C) the Mann-Whitney *U*-test. These values are associated with the arched gray lines at the top of each panel which indicate the values that were compared. The numbers of samples used to generate the plots are indicated in parentheses.

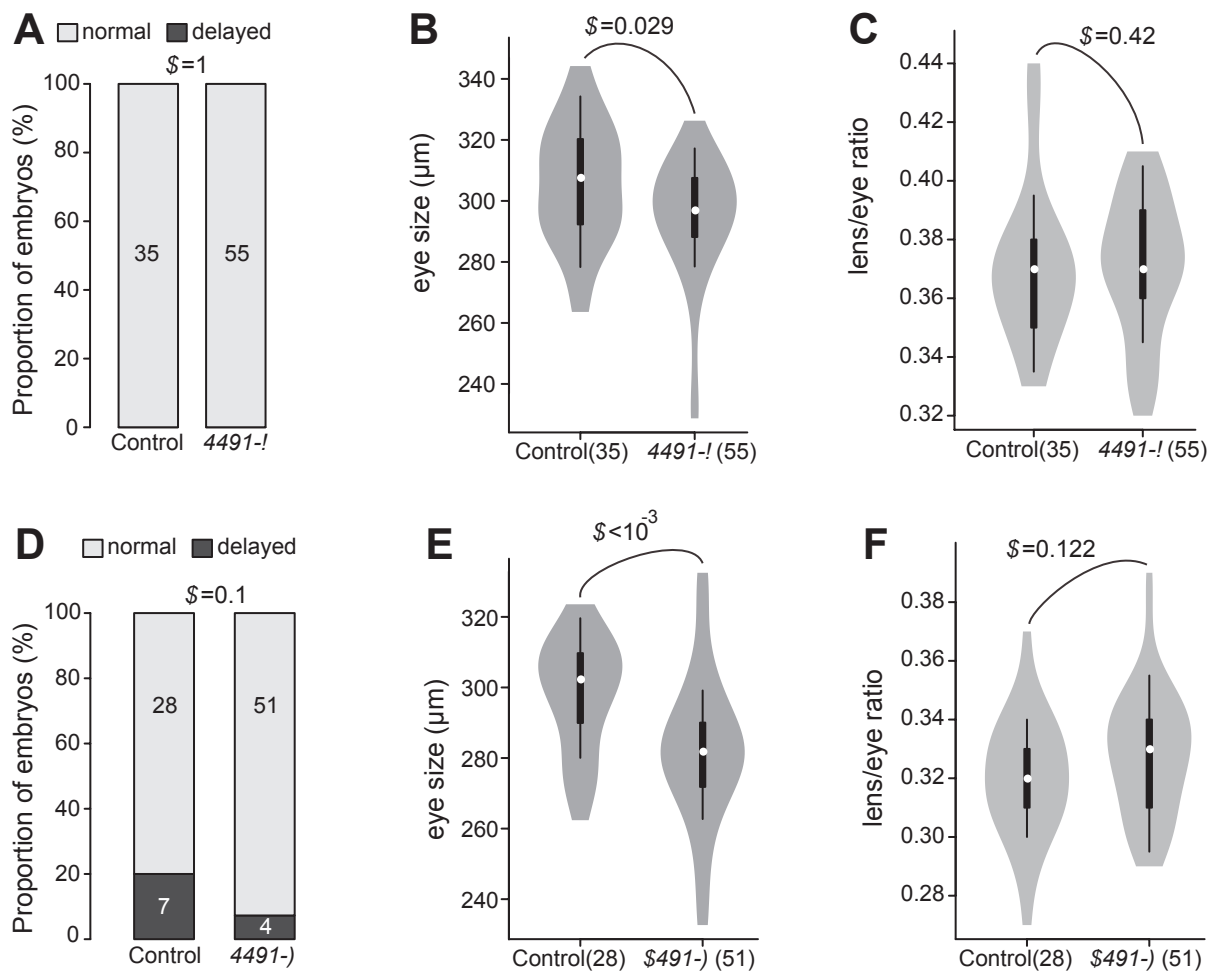


Figure S19. Consequences of knocking down the zebrafish orthologs of the mouse gene, *Ppef2*, by the groups of MO labeled “*ppef2a*” (**A-C**) and “*ppef2b*” (**D-F**). The phenotypes measured included: (**A,D**) the proportion of normal or delayed embryos, (**B,E**) eye size, and (**C,F**) lens/eye ratio. *P*-values were determined with (**A,D**) Fisher’s exact test or (**B,C,E,F**) the Mann-Whitney *U*-test. These values are associated with the arched gray lines at the top of each panel which indicate the values that were compared. The numbers of samples used to generate the plots are indicated in parentheses.

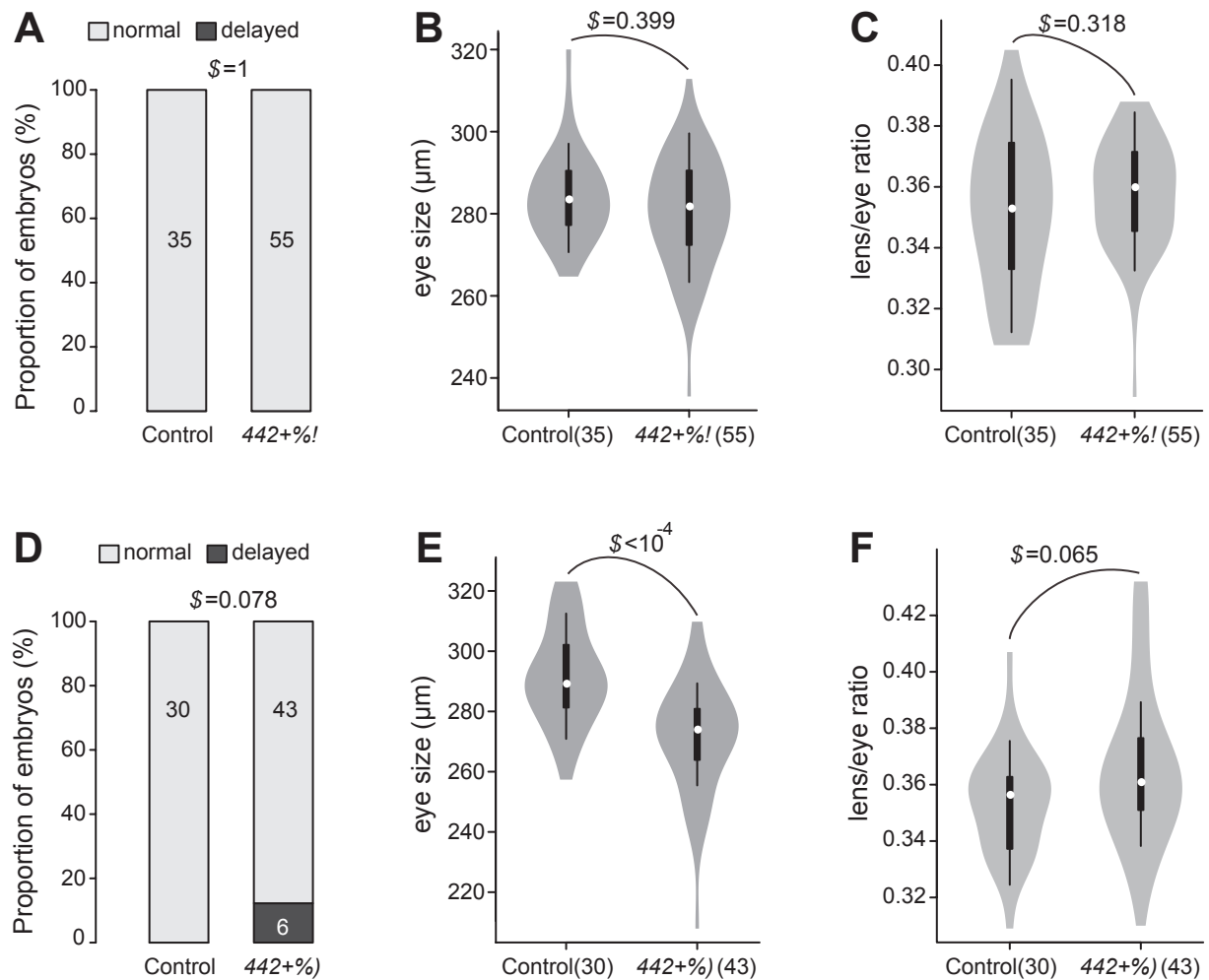


Figure S20. Consequences of knocking down the zebrafish orthologs of the mouse gene, *Ppm1n*, by the groups of MO labeled “*ppm1na*” (**A-C**) and “*ppm1nb*” (**D-F**). The phenotypes measured included: (**A,D**) the proportion of normal or delayed embryos, (**B,E**) eye size, and (**C,F**) lens/eye ratio. *P*-values were determined with (**A,D**) Fisher’s exact test or (**B,C,E,F**) the Mann-Whitney *U*-test. These values are associated with the arched gray lines at the top of each panel which indicate the values that were compared. The numbers of samples used to generate the plots are indicated in parentheses.

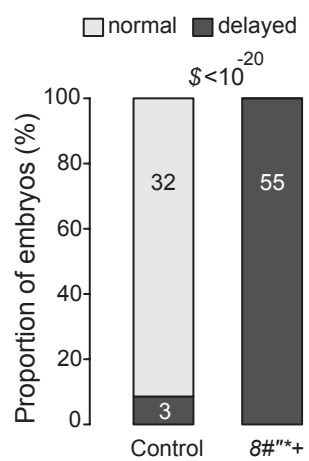


Figure S21. Consequences of knocking down the zebrafish ortholog of the mouse gene, *Tldc1*, by the group of MO labeled, “*tldc1*”. All MO-injected embryos showed developmental delay. Because only embryos developing at a normal speed were examined for the eye phenotypes, no comparison in eye morphology between the MO and the control groups was conducted. *P*-values were determined with Fisher’s exact test. The numbers of samples used to generate the plots are indicated in parentheses.

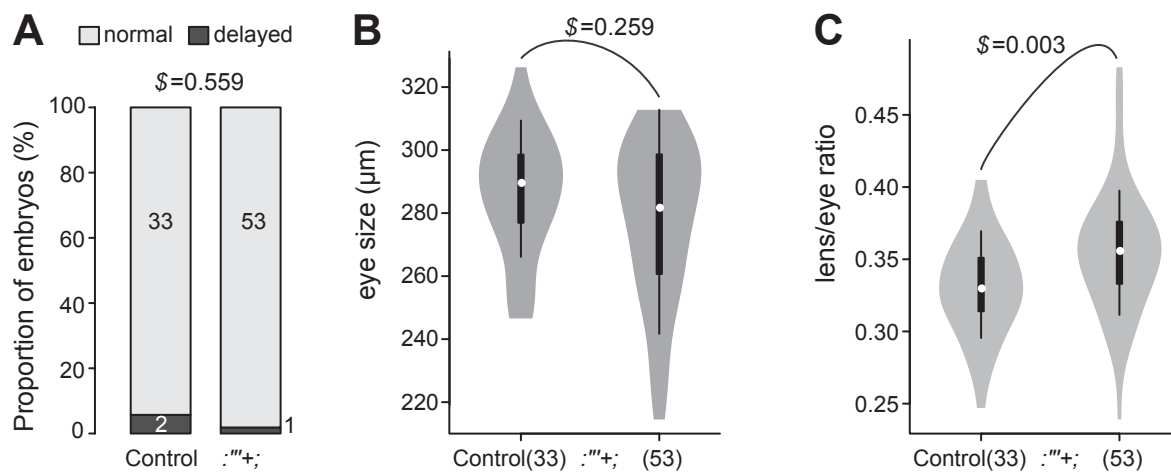


Figure S22. Consequences of knocking down the zebrafish ortholog of the mouse gene, *Wdr17*, by the group of MO labeled, “*wdr17*”. The phenotypes measured included: **(A)** the proportion of normal or delayed embryos, **(B)** eye size, and **(C)** lens/eye ratio. *P*-values were determined with **(A)** Fisher’s exact test or **(B, C)** the Mann-Whitney *U*-test. These values are associated with the arched gray lines at the top of each panel which indicate the values that were compared. The numbers of samples used to generate the plots are indicated in parentheses.

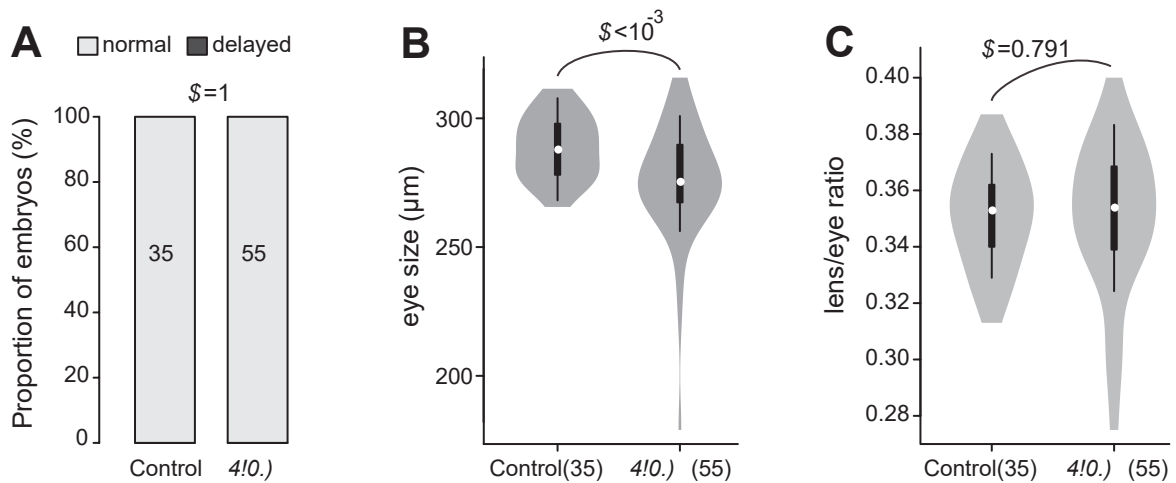


Figure S23. Consequences of knocking down the zebrafish ortholog of the mouse gene, *Pax6b*, by the group of MO labeled, “*pax6b*”. The phenotypes measured included: (A) the proportion of normal or delayed embryos, (B) eye size, and (C) lens/eye ratio. *P*-values were determined with (A) Fisher’s exact test or (B, C) the Mann-Whitney *U*-test. These values are associated with the arched gray lines at the top of each panel which indicate the values that were compared. The numbers of samples used to generate the plots are indicated in parentheses.

Table S1. The list of tissues whose transcriptomes were profiled by the microarray platform GNF1M and were used to construct the GNF1M-based gene coexpression network. Expression signals were obtained from BioGPS (<http://biogps.org/>).

Label of Tissues/Cells	Host condition	GEO Accession ¹
Osteoblasts_day5	Adult (8- to 10-week-old)	GSM286389; GSM286390
Osteoblasts_day14	Adult (8- to 10-week-old)	GSM286391; GSM286392
Osteoblasts_day21	Adult (8- to 10-week-old)	GSM286393; GSM286394
Osteoclasts	Adult (8- to 10-week-old)	GSM286395; GSM286396
Macrophage_unstimulated	Adult (8- to 10-week-old)	GSM286397; GSM286398
Macrophage_1hrIps	Adult (8- to 10-week-old)	GSM286399; GSM286400
Macrophage_7hrIps	Adult (8- to 10-week-old)	GSM286401; GSM286402
Mast cells	Adult (8- to 10-week-old)	GSM286403; GSM286404
Septal organ	Unspecified	-
Septum (resp epith)	Unspecified	-
Neuro2a	Unspecified	-
Embryonic stem feeder layer	Unspecified	-
Embryonic stem no feeder	Unspecified	-
Nih 3T3	Adult (8- to 10-week-old)	-
M-1	Adult (8- to 10-week-old)	-
C2c12	Adult (8- to 10-week-old)	-
Cerebellum	Adult (10- to 12-week-old)	GSM18606; GSM18607
Lymphnode	Adult (10- to 12-week-old)	GSM18616; GSM18617
Uterus	Adult (10- to 12-week-old)	GSM18620; GSM18621
Heart	Adult (10- to 12-week-old)	GSM18678; GSM18679
Testis	Adult (10- to 12-week-old)	GSM18704; GSM18705
Adipose tissue	Adult (10- to 12-week-old)	GSM18624; GSM18625
Adrenal gland	Adult (10- to 12-week-old)	GSM18626; GSM18627
Bladder	Adult (10- to 12-week-old)	GSM18628; GSM18629
Kidney	Adult (10- to 12-week-old)	GSM18688; GSM18689
Liver	Adult (10- to 12-week-old)	GSM18696; GSM18697
Dorsal striatum	Adult (10- to 12-week-old)	GSM18600; GSM18601
Cerebral cortex	Adult (10- to 12-week-old)	GSM18596
Frontal cortex	Adult (10- to 12-week-old)	GSM18594; GSM18595
Hippocampus	Adult (10- to 12-week-old)	GSM18602; GSM18603
Prostate	Adult (10- to 12-week-old)	GSM18650; GSM18651
Salivary gland	Adult (10- to 12-week-old)	GSM18692; GSM18693
Epidermis	Adult (10- to 12-week-old)	GSM18640; GSM18641
Umbilical cord	Adult (10- to 12-week-old)	GSM18656; GSM18657
Olfactory bulb	Adult (10- to 12-week-old)	GSM18604; GSM18605
Substantia nigra	Adult (10- to 12-week-old)	GSM18584; GSM18585
Bone	Adult (10- to 12-week-old)	GSM18664; GSM18665
Large intestine	Adult (10- to 12-week-old)	GSM18660; GSM18661
Spleen	Adult (10- to 12-week-old)	GSM18666; GSM18667
Pituitary	Adult (10- to 12-week-old)	GSM18612; GSM18613
Vomeralnasal organ.VMO.	Adult (10- to 12-week-old)	GSM18652; GSM18653
Medial olfactory epithelium	Adult (10- to 12-week-old)	GSM18648; GSM18649
Dorsal root ganglion	Adult (10- to 12-week-old)	GSM18610; GSM18611
Placenta	Adult (10- to 12-week-old)	GSM18682; GSM18683
Cd4.Tcell	Developing embryos	GSM18672; GSM18673
Cd8.Tcell	Developing embryos	GSM18674; GSM18675
B220.bcell	Developing embryos	GSM18670; GSM18671
Lung	Adult (10- to 12-week-old)	GSM18654; GSM18655
Eye	Adult (10- to 12-week-old)	GSM18614; GSM18615
Amygdala	Adult (10- to 12-week-old)	GSM18598; GSM18599
Thyroid	Adult (10- to 12-week-old)	GSM18694; GSM18695
Trigeminal	Adult (10- to 12-week-old)	GSM18608; GSM18609
Small intestine	Adult (10- to 12-week-old)	GSM18690; GSM18691
Stomach	Adult (10- to 12-week-old)	GSM18658; GSM18659
Hypothalamus	Adult (10- to 12-week-old)	GSM18590; GSM18591
Spinal cord lower	Adult (10- to 12-week-old)	GSM18588; GSM18589

Spinal cord upper	Adult (10- to 12-week-old)	GSM18586; GSM18587
Pancreas	Adult (10- to 12-week-old)	GSM18702; GSM18703
Brown fat	Adult (10- to 12-week-old)	GSM18676; GSM18677
Mammary gland.lact.	Adult (10- to 12-week-old)	GSM18684; GSM18685
Embryoday6.5	Developing embryos	GSM18638; GSM18639
Embryoday7.5	Developing embryos	GSM18636; GSM18637
Embryoday8.5	Developing embryos	GSM18634; GSM18635
Embryoday9.5	Developing embryos	GSM18632; GSM18633
Fertilizedegg	Adult (10- to 12-week-old)	GSM18698; GSM18699
Oocyte	Adult (10- to 12-week-old)	GSM18700; GSM18701
Blastocysts	Adult (10- to 12-week-old)	GSM18686; GSM18687
Embryoday10.5	Developing embryos	GSM18630; GSM18631
Digits	Adult (10- to 12-week-old)	GSM18642; GSM18643
Snoutepidermis	Adult (10- to 12-week-old)	GSM18644; GSM18645
Thymus	Adult (10- to 12-week-old)	GSM18668; GSM18669
Tongueepidermis	Adult (10- to 12-week-old)	GSM18646; GSM18647
Trachea	Adult (10- to 12-week-old)	GSM18618; GSM18619
Cortex	Adult (10- to 12-week-old)	GSM18597
Ovary	Adult (10- to 12-week-old)	GSM18622; GSM18623
Skeletalmuscle	Adult (10- to 12-week-old)	GSM18680; GSM18681
Bonemarrow	Adult (10- to 12-week-old)	GSM18662; GSM18663
Preoptic	Adult (10- to 12-week-old)	GSM18592; GSM18593

¹ Equivalent data source at NCBI GEO: <https://www.ncbi.nlm.nih.gov/geo/>

Table S2. The list of tissues whose transcriptomes were profiled by the microarray platform MOE430 2.0 and were used to construct the MOE430-based gene coexpression network. Expression signals were obtained from BioGPS (<http://biogps.org/>).

Label of Tissues/Cells	Host condition	GEO Accession ¹
3T3-L1	Adult (8- to 10-week-old)	GSM258609; GSM258610
B-cells_GL7_negative_KLH	Developing embryos	-
B-cells_GL7_positive_Alum	Unspecified	-
B-cells_GL7_positive_KLH	Unspecified	-
B-cells_GL7negative_Alum	Unspecified	-
B-cells_marginal_zone	Adult (8- to 10-week-old)	GSM258621; GSM258622
BAF3	Adult (8- to 10-week-old)	GSM258619; GSM258620
C2C12	Adult (8- to 10-week-old)	GSM258629; GSM258630
C3H_10T1_2	Adult (8- to 10-week-old)	GSM258631; GSM258632
MEF		
NK_cells	Adult (8- to 10-week-old)	GSM258731; GSM258732
Raw_264_7	Adult (8- to 10-week-old)	GSM258755; GSM258756
T-cells_CD4+	Adult (8- to 10-week-old)	GSM258773; GSM258774
T-cells_CD8+	Adult (8- to 10-week-old)	GSM258775; GSM258776
T-cells_foxp3+	Adult (8- to 10-week-old)	GSM258777; GSM258778
Adipose_brown	Adult (8- to 10-week-old)	GSM258611; GSM258612
Adipose_white	Adult (8- to 10-week-old)	GSM258613; GSM258614
Adrenal_gland	Adult (8- to 10-week-old)	GSM258615; GSM258616
Amygdala	Adult (8- to 10-week-old)	GSM258617; GSM258618
Bladder	Adult (8- to 10-week-old)	GSM258623; GSM258624
Bone	Adult (8- to 10-week-old)	GSM258625; GSM258626
Bone_marrow	Adult (8- to 10-week-old)	GSM258627; GSM258628
Cerebellum	Adult (8- to 10-week-old)	GSM258633; GSM258634
Cerebral_cortex	Adult (8- to 10-week-old)	GSM258635; GSM258636
Cerebral_cortex_prefrontal	Adult (8- to 10-week-old)	GSM258637; GSM258638
Ciliary_bodies	Adult (8- to 10-week-old)	GSM258639; GSM258640
Common_myeloid_progenitor	Adult (8- to 10-week-old)	GSM258641; GSM258642
Cornea	Adult (8- to 10-week-old)	GSM258643; GSM258644
Dendritic_cells_lymphoid_CD8a+	Adult (8- to 10-week-old)	GSM258645; GSM258646
Dendritic_cells_myeloid_CD8a-	Adult (8- to 10-week-old)	GSM258647; GSM258648
Dendritic_plasmacytoid_B220+	Adult (8- to 10-week-old)	GSM258649; GSM258650
Dorsal_root_ganglia	Adult (8- to 10-week-old)	GSM258651; GSM258652
Dorsal_striatum	Adult (8- to 10-week-old)	GSM258653; GSM258654
Embryonic_stem_line_Bruce4_p13	Adult (8- to 10-week-old)	GSM258655; GSM258656
Embryonic_stem_line_V26_2_p16	Adult (8- to 10-week-old)	GSM258657; GSM258658
Epidermis	Adult (8- to 10-week-old)	GSM258659; GSM258660
Eyecup	Adult (8- to 10-week-old)	GSM258661; GSM258662
Follicular_B-cells	Adult (8- to 10-week-old)	GSM258663; GSM258664
Granulo_mono_progenitor	Adult (8- to 10-week-old)	GSM258665; GSM258666
Granulocytes_mac1+gr1+	Adult (8- to 10-week-old)	GSM258667; GSM258668
Heart	Adult (8- to 10-week-old)	GSM258669; GSM258670
Hippocampus	Adult (8- to 10-week-old)	GSM258671; GSM258672
Hypothalamus	Adult (8- to 10-week-old)	GSM258673; GSM258674
Intestine_large	Adult (8- to 10-week-old)	GSM258675; GSM258676
Intestine_small	Adult (8- to 10-week-old)	GSM258677; GSM258678
Iris	Adult (8- to 10-week-old)	GSM258679; GSM258680
Kidney	Adult (8- to 10-week-old)	GSM258681; GSM258682
Lacrimal_gland	Adult (8- to 10-week-old)	GSM258683; GSM258684
Lens	Adult (8- to 10-week-old)	GSM258685; GSM258686
Liver	Adult (8- to 10-week-old)	GSM258687; GSM258688
Lung	Adult (8- to 10-week-old)	GSM258689; GSM258690
Lymph_nodes	Adult (8- to 10-week-old)	GSM258691; GSM258692
Mimcd-3	Adult (8- to 10-week-old)	GSM258723; GSM258724
Macrophage_bone_marrow_0hr	Adult (8- to 10-week-old)	GSM258693; GSM258694
Macrophage_bone_marrow_24h_LPS	Adult (8- to 10-week-old)	GSM258695; GSM258696

Macrophage_bone_marrow_2hr_LPS	Adult (8- to 10-week-old)	GSM258697; GSM258698
Macrophage_bone_marrow_6hr_LPS	Adult (8- to 10-week-old)	GSM258699; GSM258700
Macrophage_peri_LPS_thio_0hrs	Adult (8- to 10-week-old)	GSM258701; GSM258702
Macrophage_peri_LPS_thio_1hrs	Adult (8- to 10-week-old)	GSM258703; GSM258704
Macrophage_peri_LPS_thio_7hrs	Adult (8- to 10-week-old)	GSM258705; GSM258706
Mammary_gland_lact	Adult (8- to 10-week-old)	GSM258707; GSM258708
Mammary_gland_non-lactating	Adult (8- to 10-week-old)	GSM258709; GSM258710
Mast_cells	Adult (8- to 10-week-old)	GSM258711; GSM258712
Mast_cells_ige	Adult (8- to 10-week-old)	GSM258713; GSM258714
Mast_cells_ige+antigen_1hr	Adult (8- to 10-week-old)	GSM258715; GSM258716
Mast_cells_ige+antigen_6hr	Adult (8- to 10-week-old)	GSM258717; GSM258718
Mega_erythrocyte_progenitor	Adult (8- to 10-week-old)	GSM258719; GSM258720
Microglia	Adult (8- to 10-week-old)	GSM258721; GSM258722
MIN6	Adult (8- to 10-week-old)	GSM258725; GSM258726
Neuro2a	Adult (8- to 10-week-old)	GSM258727; GSM258728
NIH_3T3	Adult (8- to 10-week-old)	GSM258729; GSM258730
Nucleus_accumbens	Adult (8- to 10-week-old)	GSM258733; GSM258734
Olfactory_bulb	Adult (8- to 10-week-old)	GSM258735; GSM258736
Osteoblast_day14	Adult (8- to 10-week-old)	GSM258737; GSM258738
Osteoblast_day21	Adult (8- to 10-week-old)	GSM258739; GSM258740
Osteoblast_day5	Adult (8- to 10-week-old)	GSM258741; GSM258742
Osteoclasts	Adult (8- to 10-week-old)	GSM258743; GSM258744
Ovary	Adult (8- to 10-week-old)	GSM258745; GSM258746
Pancreas	Adult (8- to 10-week-old)	GSM258747; GSM258748
Pituitary	Adult (8- to 10-week-old)	GSM258749; GSM258750
Placenta	Adult (8- to 10-week-old)	GSM258751; GSM258752
Prostate	Adult (8- to 10-week-old)	GSM258753; GSM258754
Eye	Adult (8- to 10-week-old)	GSM258757; GSM258758
Eyel_pigment_epithelium	Adult (8- to 10-week-old)	GSM258759; GSM258760
Salivary_gland	Adult (8- to 10-week-old)	GSM258761; GSM258762
Skeletal_muscle	Adult (8- to 10-week-old)	GSM258763; GSM258764
Spinal_cord	Adult (8- to 10-week-old)	GSM258765; GSM258766
Spleen	Adult (8- to 10-week-old)	GSM258767; GSM258768
Stem_cells_HSC	Adult (8- to 10-week-old)	GSM258769; GSM258770
Stomach	Adult (8- to 10-week-old)	GSM258771; GSM258772
Testis	Adult (8- to 10-week-old)	GSM258779; GSM258780
Thymocyte_DP_CD4+CD8+	Adult (8- to 10-week-old)	GSM258781; GSM258782
Thymocyte_SP_CD4+	Adult (8- to 10-week-old)	GSM258783; GSM258784
Thymocyte_SP_CD8+	Adult (8- to 10-week-old)	GSM258785; GSM258786
Umbilical_cord	Adult (8- to 10-week-old)	GSM258787; GSM258788
Uterus	Adult (8- to 10-week-old)	GSM258789; GSM258790

¹ Equivalent data source at NCBI GEO: <https://www.ncbi.nlm.nih.gov/geo/>

Table S3. The list of tissues whose transcriptomes were profiled by the RNA-seq and were used to construct the RNA-seq-based gene coexpression network. Expression signals were processed and normalized as described in Materials and Methods.

Label of Tissues/Cells	Host condition	GEO Accession ¹
Adrenal	Adult (8-week-old)	GSM900188
Bladder	Adult (8-week-old)	GSM1000564
Cerebellum	Adult (8-week-old)	GSM1000567
CNS115	E11.5 embryo	GSM1000573
CNS14	E14 embryo	GSM1000569
CNS18	E18 embryo	GSM1000570
Colon	Adult (8-week-old)	GSM900198
Cortex	Adult (8-week-old)	GSM1000563
Duodenum	Adult (8-week-old)	GSM900187
Frontal lobe	Adult (8-week-old)	GSM1000562
Genital Fat Pad	Adult (8-week-old)	GSM900190
Heart	Adult (8-week-old)	GSM900199
Kidney	Adult (8-week-old)	GSM900194
Large Intestine	Adult (8-week-old)	GSM900189
LimbE145	E14.5 embryo	GSM1000568
Liver	Adult (8-week-old)	GSM900195
LiverE14	E14 embryo	GSM1000574
LiverE145	E14.5 embryo	GSM1000571
LiverE18	E18 embryo	GSM1000566
Lung	Adult (8-week-old)	GSM900196
Mammary Gland	Adult (8-week-old)	GSM900184
Ovary	Adult (8-week-old)	GSM900183
Placenta	Adult (8-week-old)	GSM1000565
Subcutaneous Fat	Adult (8-week-old)	
Pad		GSM900191
Small Intestine	Adult (8-week-old)	GSM900186
Spleen	Adult (8-week-old)	GSM900197
Stomach	Adult (8-week-old)	GSM900185
Testis	Adult (8-week-old)	GSM900193
Thymus	Adult (8-week-old)	GSM900192
Whole brain E14.5	E14.5 embryo	GSM1000572
Eye	4-week-old	GSM737550
Spinal cord	Adult (10- to 16-week-old)	GSM1103369; GSM1103370
Dorsal root ganglia	-	GSM1150934; GSM1150935; GSM1150936
Trigeminal	-	GSM1150931; GSM1150932; GSM1150933
Adipose tissue	1-week-old	GSM1321366; GSM1321367; GSM1321368; GSM1321369; GSM1321370; GSM1321371; GSM1321372; GSM1321373
Skeletal muscle	-	GSM1322910; GSM1322911; GSM1322912
Brown fat	Adult (3-month-old)	GSM1359961; GSM1359962; GSM1359963
Medial olfactory epithelium	Adult (age unspecified)	GSE57567
Hippocampus	Adult (3-month-old)	GSM1517288; GSM1517289; GSM1517290; GSM1517291; GSM1517292
Tongue	Adult (31-week-old)	GSM1520071; GSM1520072; GSM1520073
Substantia nigra	-	GSM1571336; GSM1571337; GSM1571338; GSM1571339; GSM1571340; GSM1571341
Pancreas	10-14 weeks	GSM1660657; GSM1660658; GSM1660659
Uterus	Adult (day 8 of pregnancy)	GSM1690181; GSM1690182
Oocyte	5- to 20-day-old	GSM1717218; GSM1717219
Hypothalamus	Adult (10- to 12-week-old)	GSM1855239; GSM1855240; GSM1855241; GSM1855242; GSM1855243; GSM1855244; GSM1855245; GSM1855246; GSM1855247
Amygdala	Adult (age unspecified)	GSM1924705; GSM1924706; GSM1924707

Prostate	Adult (4-month-old)	GSM2152244; GSM2152245; GSM2152246; GSM2152247; GSM2152248; GSM2152249
Olfactory bulb	Adult (age unspecified)	GSM1100706
Epidermis	Adult (10-week-old)	GSM1410794
Lymph node	Adult (10- to 12-week-old)	GSM1680970
Thyroid	Adult (6-month-old)	GSM652441
Bone marrow	Adult (8-week-old)	GSM723767
Dorsal striatum	Adult (3-month-old)	GSM884357

¹ Data available from the NCBI GEO: <https://www.ncbi.nlm.nih.gov/geo/>

Table S4. The 47 mouse tissues used to functionally annotate gene modules and their corresponding tissue names, presented as MA codes, in MGI for the records of mutant strain phenotyping. The substructures of each tissue (in MA codes) and the associated phenotypic codes (in MP IDs) are provided as Dataset S1.

#	Tissue	Tissue name (MA code) in MGI
1	Adipose tissue	Adipose tissue (MA:0000009)
2	Adrenal gland	Adrenal gland (MA:0000116)
3	Amygdala	Amygdala (MA:0000887)
4	Bladder	Urinary bladder (MA:0000380)
5	Bone	Bone (MA:0001459)
6	Bone marrow	Bone marrow (MA:0000134)
7	Brown fat	Brown adipose tissue (MA:0000057)
8	Cerebellum	Cerebellum (MA:0000198)
9	Cerebral cortex	Cerebral cortex (MA:0000185)
10	Digits	Limb digit (MA:0000690)
11	Dorsal root ganglia	Dorsal root ganglion (MA:0000232)
12	Dorsal striatum	Dorsal striatum (MA:0002971)
13	Epidermis	Epidermis (MA:0000153)
14	Eye	Eye (MA:0000261)
15	Frontal cortex	Frontal cortex (MA:0000905)
16	Heart	Heart (MA:0000072)
17	Hippocampus	Hippocampus (MA:0000191)
18	Hypothalamus	Hypothalamus (MA:0000173)
19	Kidney	Kidney (MA:0000368)
20	Large intestine	Large intestine (MA:0000333)
21	Liver	Liver (MA:0000358)
22	Lung	Lung (MA:0000415)
23	Lymph node	Lymph node (MA:0000139)
24	Mammary gland	Mammary gland (MA:0000145)
25	Medial olfactory epithelium	Nasal cavity olfactory epithelium (MA:0001325)
26	Olfactory bulb	Main olfactory bulb (MA:0000194)
27	Oocyte	Oocyte (MA:0000388)
28	Ovary	Ovary (MA:0000384)
29	Pancreas	Pancreas (MA:0000120)
30	Pituitary	Pituitary gland (MA:0000176)
31	Placenta	Placenta (MA:0000386)
32	Prostate	Prostate gland (MA:0000404)
33	Salivary gland	Salivary gland (MA:0000346)
34	Skeletal muscle	Skeletal muscle tissue (MA:0002439)
35	Small intestine	Small intestine (MA:0000337)
36	Spinal cord, lower and upper	Spinal cord (MA:0000216)
37	Spleen	Spleen (MA:0000141)
38	Stomach	Stomach (MA:0000353)
39	Substantia nigra	Substantia nigra (MA:0000210)
40	Testis	Testis (MA:0000411)
41	Thymus	Thymus (MA:0000142)
42	Thyroid	Thyroid gland (MA:0000129)
43	Tongue	Tongue (MA:0000347)
44	Trachea	Trachea (MA:0000441)
45	Trigeminal	Trigeminal V nerve (MA:0001100)
46	Uterus	Uterus (MA:0000389)
47	Vomeronasal organ	Vomeronasal organ (MA:0000289)

Table S5. Gene modules in the GNF1M-based coexpression network and the associated tissue identified by enrichment analysis based on mutant phenotypes for each module. The graph of the modular structures is presented as Figure S3.

Module ID	Number of genes	Number of phenotyped genes	Associated tissue type (\$ value)
1	2584	620	
2	1475	348	ovary ($<10^{-3}$)
3	1444	208	testis ($<10^{-23}$); oocyte ($<10^{-6}$)
4	842	216	hippocampus ($<10^{-13}$); cerebral cortex ($<10^{-6}$); cerebellum ($<10^{-6}$); frontal cortex ($<10^{-3}$); spinal cord ($<10^{-3}$)
5	837	163	placenta ($<10^{-6}$); testis ($<10^{-3}$)
6	591	201	spleen ($<10^{-7}$)
7	468	148	lymph node ($<10^{-15}$); spleen ($<10^{-11}$); thyroid ($<10^{-11}$); thymus ($<10^{-11}$); bone marrow ($<10^{-6}$)
8	423	113	
9	393	176	bone ($<10^{-5}$)
10	372	118	liver ($<10^{-18}$)
11	271	79	skeletal muscle ($<10^{-7}$); bone ($<10^{-2}$)
12	269	76	kidney ($<10^{-12}$)
13	268	87	lymph node ($<10^{-6}$); bone marrow ($<10^{-4}$); bone ($<10^{-3}$)
14	252	63	hypothalamus ($<10^{-4}$)
15	243	80	bone marrow ($<10^{-9}$); spleen ($<10^{-4}$)
16	228	63	epidermis ($<10^{-10}$); tongue ($<10^{-3}$)
17	223	52	spinal cord ($<10^{-3}$)
18	220	62	cerebellum ($<10^{-3}$); spinal cord ($<10^{-3}$)
19	215	51	medial olfactory epithelium ($<10^{-5}$); olfactory bulb ($<10^{-5}$)
20	213	57	small intestine ($<10^{-5}$)
21	209	67	skeletal muscle ($<10^{-19}$)
22	198	68	spleen ($<10^{-17}$); lymph node ($<10^{-7}$)
23	196	52	
24	193	44	heart ($<10^{-14}$)
25	185	101	eye ($<10^{-37}$)
26	183	67	thymus ($<10^{-11}$); thyroid ($<10^{-10}$)
27	181	94	lung ($<10^{-7}$); heart ($<10^{-3}$)
28	164	54	large intestine ($<10^{-7}$)
29	155	48	
30	146	37	
31	137	33	placenta ($<10^{-3}$)
32	122	35	cerebellum ($<10^{-8}$)
33	117	46	
34	104	31	prostate ($<10^{-3}$)
35	104	42	adipose tissue ($<10^{-8}$); brown fat ($<10^{-6}$); liver ($<10^{-4}$); pancreas ($<10^{-3}$)
36	97	26	
37	95	48	lung ($<10^{-4}$)
38	87	42	spleen ($<10^{-6}$); large intestine ($<10^{-4}$); bone ($<10^{-3}$); bone marrow ($<10^{-3}$)
39	87	33	adrenal gland ($<10^{-6}$)
40	86	27	tongue ($<10^{-3}$)
41	84	32	bone marrow ($<10^{-5}$); bone ($<10^{-4}$); spleen ($<10^{-3}$)
42	76	31	stomach ($<10^{-14}$)
43	69	35	
44	69	25	mammary gland ($<10^{-10}$)
45	69	20	
46	68	16	
47	58	15	brown fat ($<10^{-4}$)
48	55	22	
49	54	21	
50	49	15	vomeronasal organ ($<10^{-5}$)

51	48	19	pituitary ($<10^{-8}$); uterus ($<10^{-4}$); adrenal gland ($<10^{-3}$)
52	40	18	placenta ($<10^{-5}$)
53	40	8	
54	36	19	

Table S6. Gene modules in the MOE430-based coexpression network and the associated tissue identified by enrichment analysis based on mutant phenotypes for each module. The graph of the modular structures is presented as Figure S4.

Module ID	Number of genes	Number of phenotyped genes	Associated tissue type (\$ value)
1	1893	307	testis ($<10^{-29}$); oocyte ($<10^{-5}$)
2	1456	296	placenta ($<10^{-11}$); testis ($<10^{-4}$); oocyte ($<10^{-3}$)
3	1171	276	hippocampus ($<10^{-11}$); cerebral cortex ($<10^{-10}$); frontal cortex ($<10^{-6}$); cerebellum ($<10^{-6}$); spinal cord ($<10^{-3}$); olfactory bulb ($<10^{-3}$)
4	942	299	spleen ($<10^{-6}$); liver ($<10^{-4}$); bone marrow ($<10^{-4}$); thymus ($<10^{-3}$)
5	641	169	thyroid ($<10^{-3}$); thymus ($<10^{-3}$); lymph node ($<10^{-3}$); bone marrow ($<10^{-3}$)
6	607	191	liver ($<10^{-20}$)
7	471	197	bone ($<10^{-8}$); digits ($<10^{-5}$); lung ($<10^{-3}$); trachea ($<10^{-3}$)
8	444	141	skeletal muscle ($<10^{-24}$); heart ($<10^{-3}$)
9	355	54	
10	331	113	spleen ($<10^{-11}$); lymph node ($<10^{-6}$)
11	323	93	kidney ($<10^{-14}$)
12	320	105	spleen ($<10^{-3}$); bone marrow ($<10^{-3}$)
13	299	43	
14	257	83	large intestine ($<10^{-7}$)
15	233	75	placenta ($<10^{-9}$)
16	223	63	small intestine ($<10^{-3}$)
17	223	52	prostate ($<10^{-3}$)
18	213	62	eye ($<10^{-4}$)
19	210	56	
20	199	48	spinal cord ($<10^{-4}$); dorsal root ganglia ($<10^{-3}$); trigeminal ($<10^{-3}$)
21	197	73	bone marrow ($<10^{-11}$); spleen ($<10^{-6}$); epidermis ($<10^{-4}$)
22	196	77	
23	191	90	heart ($<10^{-6}$); lung ($<10^{-6}$)
24	189	51	cerebellum ($<10^{-6}$); hippocampus ($<10^{-3}$); spinal cord ($<10^{-3}$)
25	188	57	bone marrow ($<10^{-3}$)
26	185	45	epidermis ($<10^{-7}$); tongue ($<10^{-3}$)
27	184	63	lymph node ($<10^{-4}$)
28	182	70	bone marrow ($<10^{-5}$); bone ($<10^{-5}$); spleen ($<10^{-5}$)
29	178	66	eye ($<10^{-21}$)
30	170	50	brown fat ($<10^{-10}$); adipose tissue ($<10^{-9}$); liver ($<10^{-6}$)
31	156	39	pancreas ($<10^{-7}$)
32	138	39	cerebellum ($<10^{-7}$)
33	130	40	
34	125	47	pancreas ($<10^{-11}$)
35	114	29	
36	112	35	
37	111	32	
38	109	38	thymus ($<10^{-12}$); thyroid ($<10^{-11}$); lymph node ($<10^{-7}$); spleen ($<10^{-5}$)
39	107	52	heart ($<10^{17}$)
40	102	23	
41	98	25	
42	97	29	stomach ($<10^{-15}$)
43	93	33	eye ($<10^{-3}$)
44	92	19	
45	92	34	bladder ($<10^{-3}$)
46	88	26	
47	83	19	
48	83	39	spleen ($<10^{-3}$)
49	74	17	hypothalamus ($<10^{-6}$)
50	69	23	
51	67	29	pituitary ($<10^{-9}$); adrenal gland ($<10^{-3}$)
52	65	33	hypothalamus ($<10^{-3}$); eye ($<10^{-3}$)

53	65	27	adrenal gland ($<10^{-3}$)
54	61	14	
55	61	19	thymus ($<10^{-5}$); thyroid ($<10^{-5}$); lymph node ($<10^{-3}$)
56	61	26	ovary ($<10^{-12}$); oocyte ($<10^{-6}$); uterus ($<10^{-4}$)
57	55	14	
58	53	20	
59	53	22	
60	47	21	
61	45	22	
62	39	15	
63	37	18	mammary gland ($<10^{-10}$)
64	30	9	

Table S7. Genes modules in the RNA-seq-based coexpression network and the associated tissue identified by enrichment analysis based on mutant phenotypes for each module. The graph of the modular structures is presented as Figure S5.

Module ID	Number of genes	Number of phenotyped genes	Associated tissue type (! value)!
1	9983	2695	Uncalculated because gene number > 5,000
2	838	245	cerebellum ($<10^{-3}$)
3	737	226	
4	570	205	spleen ($<10^{-26}$); lymph node ($<10^{-25}$); large intestine ($<10^{-7}$); thymus ($<10^{-5}$); thyroid ($<10^{-4}$); bone marrow ($<10^{-4}$)
5	478	102	
6	449	120	spleen ($<10^{-4}$); lymph node ($<10^{-4}$); thymus ($<10^{-4}$); thyroid ($<10^{-3}$)
7	416	92	
8	306	122	eye ($<10^{-27}$)
9	292	110	skeletal muscle ($<10^{-5}$)
10	248	72	cerebral cortex ($<10^{-4}$); olfactory bulb ($<10^{-3}$); hippocampus ($<10^{-3}$)
11	241	56	
12	227	71	
13	170	54	hypothalamus ($<10^{-3}$)
14	136	44	
15	133	8	
16	127	34	olfactory bulb ($<10^{-3}$)
17	123	7	
18	94	31	
19	87	21	
20	66	14	bladder ($<10^{-3}$); prostate ($<10^{-3}$)
21	41	15	
22	34	17	

Table S8. The module IDs that were associated with any of the 47 mouse tissues for each of the GNF1M-, MOE430- or RNA-seq-based network.

#	Tissue	Associated modules IDs in the network		
		GNF1M	MOE430	RNA-seq
1	Adipose tissue	35	30	
2	Adrenal gland	39, 51	51, 53	
3	Amygdala			
4	Bladder		45	20
5	Bone	9, 11, 13, 38, 41	7, 28	
6	Bone marrow	7, 13, 15, 38, 41	4, 5, 12, 21, 25, 28	4
7	Brown fat	35, 47	30	
8	Cerebellum	4, 18, 32	3, 24, 32	2
9	Cerebral cortex	4	3	10
10	Digits		7	
11	Dorsal root ganglia		20	
12	Dorsal striatum			
13	Epidermis	16	21, 26	
14	Eye	25	18, 29, 43, 52	8
15	Frontal cortex	4	3	
16	Heart	24, 27	8, 23, 39	
17	Hippocampus	4	3, 24	10
18	Hypothalamus	14	49, 52	13
19	Kidney	12	11	
20	Large intestine	28, 38	14	4
21	Liver	10, 35	4, 6, 30	
22	Lung	27, 37	7, 23	
23	Lymph node	7, 13, 22	5, 10, 27, 38, 55	4, 6
24	Mammary gland	44	63	
25	Medial olfactory epithel.	19		
26	Olfactory bulb	19	3	10, 16
27	Oocyte	3	1, 2, 56	
28	Ovary	2	56	
29	Pancreas	35	31, 34	
30	Pituitary	51	51	
31	Placenta	5, 31, 52	2, 15	
32	Prostate	34	17	20
33	Salivary gland			
34	Skeletal muscle	11, 21	8	9
35	Small intestine	20	16	
36	Spinal cord	4, 17, 18	3, 20, 24	
37	Spleen	6, 7, 15, 22, 38, 41	4, 10, 12, 21, 28, 38, 48	4, 6
38	Stomach	42	42	
39	Substantia nigra			
40	Testis	3, 5	1, 2	
41	Thymus	7, 26	4, 5, 38, 55	4, 6
42	Thyroid	7, 26	5, 38, 55	4, 6
43	Tongue	16, 40	26	
44	Trachea		7	
45	Trigeminal		20	
46	Uterus	51	56	
47	Vomeronasal organ	50		

Table S9. $R_{dcv/phe}$ for each set of genes with a given confidence score and a given predicted tissue function.

Predicted tissue function	Confidence score of genes			
	High	Medium	Low	Others
Adipose tissue	-	58.82% (10/17)	43.1% (25/58)	11.46% (491/4284)
Adrenal gland	-	26.47% (9/34)	10% (4/40)	1.82% (78/4285)
Amygdala	-	-	-	0.18% (8/4359)
Bladder	-	100% (1/1)	10.87% (5/46)	0.95% (41/4312)
Bone	57.45% (27/47)	53.57% (195/364)	40.46% (384/949)	28.71% (861/2999)
Bone marrow	31.11% (14/45)	31.39% (70/223)	18.85% (148/785)	6.9% (228/3306)
Brown fat	-	33.33% (8/24)	18.64% (11/59)	1.78% (76/4276)
Cerebellum	26.67% (8/30)	21.26% (44/207)	8.81% (37/420)	4.24% (157/3702)
Cerebral cortex	50% (2/4)	16.28% (21/129)	10.54% (31/294)	3.64% (143/3932)
Digits	-	-	11.17% (22/197)	3.92% (163/4162)
Dorsal root ganglia	-	-	12.5% (6/48)	1.51% (65/4311)
Dorsal striatum	-	-	-	0.14% (6/4359)
Epidermis	-	71.43% (15/21)	33.81% (47/139)	13.05% (548/4199)
Eye	96.30% (52/54)	77.27% (34/44)	34.39% (65/189)	19.25% (784/4072)
Frontal cortex	-	3.2% (4/125)	2.07% (5/242)	0.1% (4/3992)
Heart	-	51.22% (42/82)	39.69% (102/257)	16.99% (683/4020)
Hippocampus	75% (3/4)	19.72% (28/142)	12.54% (40/319)	3.65% (142/3894)
Hypothalamus	100% (1/1)	40% (4/10)	6.29% (9/143)	0.67% (28/4205)
Kidney	-	56.25% (27/48)	36.99% (27/73)	13.1% (555/4238)
Large intestine	0% (0/1)	31.91% (15/47)	12.89% (37/287)	3.16% (127/4024)
Liver	-	57.36% (74/129)	30.39% (134/441)	15.54% (589/3789)
Lung	-	40.98% (25/61)	23.78% (73/307)	11.48% (458/3991)
Lymph node	50.88% (29/57)	23.08% (36/156)	10.6% (58/547)	2.64% (95/3599)
Mammary gland	-	69.23% (9/13)	17.65% (3/17)	2.84% (123/4329)
Medial olfactory epithelium	-	-	11.76% (6/51)	0.65% (28/4308)
Olfactory bulb	100% (1/1)	23.08% (3/13)	6.68% (27/404)	1.55% (61/3941)
Oocyte	-	9.09% (14/154)	5.29% (28/529)	0.9% (33/3676)
Ovary	-	90% (9/10)	8.19% (29/354)	4.63% (185/3995)
Pancreas	-	-	34.38% (44/128)	5.51% (233/4231)
Pituitary	-	57.14% (8/14)	10% (2/20)	1.92% (83/4325)
Placenta	-	28.57% (40/140)	15.46% (47/304)	5.72% (224/3915)
Prostate	-	20% (1/5)	11.49% (10/87)	1.12% (48/4267)
Salivary gland	-	-	-	1.65% (72/4359)
Skeletal muscle	78.57% (11/14)	48.28% (28/58)	14.23% (34/239)	5.16% (209/4048)
Small intestine	-	20% (6/30)	6.67% (4/60)	2.25% (96/4269)
Spinal cord	-	14.43% (29/201)	10.56% (32/303)	3.99% (154/3855)
Spleen	60.87% (56/92)	37.32% (128/343)	22.69% (152/670)	9.25% (301/3254)
Stomach	-	58.82% (10/17)	33.33% (8/24)	2.62% (113/4318)
Substantia nigra	-	-	-	0.21% (9/4359)
Testis	-	32.58% (86/264)	18.61% (83/446)	7.23% (264/3649)
Thymus	60% (24/40)	27.83% (32/115)	11.34% (81/714)	5.76% (201/3490)
Thyroid	58.06% (18/31)	38.16% (29/76)	12.09% (63/521)	6.33% (236/3731)
Tongue	-	10% (2/20)	11.58% (11/95)	1.23% (52/4244)
Trachea	-	-	4.57% (9/197)	0.94% (39/4162)
Trigeminal	-	-	10.42% (5/48)	1.25% (54/4311)
Uterus	-	-	26.67% (12/45)	2.74% (118/4314)
Vomeronasal organ	-	-	-	0.21% (9/4359)

Table S10. Enrichment of human orthologs of mouse genes with the top ranked Z_{eye} in genes cataloged in RetNet (dubbed “RetNet”) or HPO-defined eye disease genes (dubbed “HPO”).

Confidence score of predicted eye functions (sample size)	P-value ¹			
	All orthologs		Orthologs without any previously reported eye phenotype in mice	
	RetNet	HPO	RetNet	HPO
High (42)	0.053	0.034	0.297	0.323
High+Medium (177)	0.016	<10 ⁻³	0.747	0.844
High+Medium+Low (821)	0.160	<10 ⁻³	0.111	ns

¹ P-value was obtained under the null hypothesis of no enrichment by Fisher's exact test (ns: not significant)

Table S11. Mouse genes whose predicted eye functions were supported by all the three datasets (i.e., with a high confidence score).

MGI ID	Gene symbol	Gene name	Mutant Strain Availability	Eye abnormality	Tissues affected by the mutations ¹
MGI:109424	Abca4	ATP-binding cassette, sub-family A (ABC1), member 4	Yes	Yes	epidermis, eye
MGI:2148800	Aipl1	aryl hydrocarbon receptor-interacting protein-like 1	Yes	Yes	eye
MGI:2443398	Ankrd33	ankyrin repeat domain 33	No	-	-
MGI:2159617	Arr3	arrestin 3, retinal	Yes	-	-
MGI:2385061	BC027072	cDNA sequence BC027072	Yes	Yes	eye
MGI:1920910	Cabp4	calcium binding protein 4	Yes	Yes	eye
MGI:1352746	Cabp5	calcium binding protein 5	Yes	Yes	eye
MGI:2442632	Cacna2d4	calcium channel, voltage-dependent, alpha 2/delta subunit 4	Yes	Yes	eye
MGI:88436	Cnga1	cyclic nucleotide gated channel alpha 1	No	-	-
MGI:2384571	Cplx3	complexin 3	Yes	Yes	eye
MGI:2685803	Cplx4	complexin 4	Yes	Yes	eye
MGI:1194883	Crx	cone-rod homeobox containing gene	Yes	Yes	eye
MGI:88515	Cryaa	crystallin, alpha A	Yes	Yes	eye
MGI:88518	Cryba1	crystallin, beta A1	Yes	Yes	eye
MGI:102716	Cryba4	crystallin, beta A4	No	-	-
MGI:88519	Crybb2	crystallin, beta B2	Yes	Yes	cerebellum, eye
MGI:102717	Crybb3	crystallin, beta B3	No	-	-
MGI:88521	Cryga	crystallin, gamma A	Yes	Yes	eye
MGI:88522	Crygb	crystallin, gamma B	Yes	Yes	eye
MGI:88524	Crygd	crystallin, gamma D	Yes	Yes	eye
MGI:88526	Crygf	crystallin, gamma F	Yes	Yes	eye
MGI:1298216	Crygs	crystallin, gamma S	Yes	Yes	eye
MGI:102563	Dct	dopachrome tautomerase	Yes	Yes	eye
MGI:95625	Gabrr1	gamma-aminobutyric acid (GABA) C receptor, subunit rho 1	Yes	Yes	eye
MGI:95626	Gabrr2	gamma-aminobutyric acid (GABA) C receptor, subunit rho 2	Yes	No	heart, testis
MGI:3648918	Gm4792	predicted gene 4792	Yes	-	-
MGI:3646315	Gm9918	predicted gene 9918	No	-	-
MGI:95778	Gnat1	guanine nucleotide binding protein, alpha transducing 1	Yes	Yes	eye
MGI:95779	Gnat2	guanine nucleotide binding protein, alpha transducing 2	Yes	Yes	eye
MGI:109165	Gngt1	guanine nucleotide binding protein (G protein), gamma transducing activity polypeptide 1	Yes	Yes	eye
MGI:1925248	Grifin	galectin-related inter-fiber protein	No	-	-
MGI:1345146	Grk1	G protein-coupled receptor kinase 1	Yes	Yes	eye
MGI:102770	Guca1a	guanylate cyclase activator 1a (retina)	Yes	Yes	eye
MGI:1194489	Guca1b	guanylate cyclase activator 1B	Yes	Yes	eye
MGI:2384820	Kcnj14	potassium inwardly-rectifying channel, subfamily J, member 14	Yes	No	-
MGI:2670981	Kcnv2	potassium channel, subfamily V, member 2	Yes	No	-
MGI:2385320	Lrit1	leucine-rich repeat, immunoglobulin-like and transmembrane domains 1	No	-	-
MGI:2444885	Lrit2	leucine-rich repeat, immunoglobulin-like and transmembrane domains 2	No	-	-
MGI:96990	Mip	major intrinsic protein of eye lens fiber	Yes	Yes	eye
MGI:108454	Mlana	melan-A	Yes	No	-

MGI:2386681	Mpp4	membrane protein, palmitoylated 4 (MAGUK p55 subfamily member 4)	Yes	Yes	eye
MGI:108055	Neurod4	neurogenic differentiation 4	Yes	No	cerebellum
MGI:1346317	Nr2e3	nuclear receptor subfamily 2, group E, member 3	Yes	Yes	eye
MGI:97454	Oca2	oculocutaneous albinism II	Yes	Yes	adipose tissue, epidermis, eye, kidney, liver, spleen, testis
MGI:1097692	Opn1mw	opsin 1 (cone pigments), medium-wave-sensitive (color blindness, deutan)	Yes	Yes	eye
MGI:97451	Otx2	orthodenticle homolog 2 (Drosophila)	Yes	Yes	bone, eye, heart, medial olfactory epithelium, olfactory bulb, pituitary, skeletal muscle, testis, tongue, trigeminal, vomerinasal organ
MGI:98090	Pdc	phosducin	Yes	Yes	eye, heart
MGI:97524	Pde6a	phosphodiesterase 6A, cGMP-specific, rod, alpha	Yes	Yes	eye
MGI:97525	Pde6b	phosphodiesterase 6B, cGMP, rod receptor, beta polypeptide	Yes	Yes	eye
MGI:105956	Pde6c	phosphodiesterase 6C, cGMP specific, cone, alpha prime	Yes	Yes	eye
MGI:97526	Pde6g	phosphodiesterase 6G, cGMP-specific, rod, gamma	Yes	Yes	eye
MGI:1925850	Pde6h	phosphodiesterase 6H, cGMP-specific, cone, gamma	Yes	No	-
MGI:1342304	Ppef2	protein phosphatase, EF hand calcium-binding domain 2	Yes	No	-
MGI:2142330	Ppm1n	protein phosphatase, Mg2+/Mn2+ dependent, 1N (putative)	No	-	-
MGI:102791	Prph2	peripherin 2	Yes	Yes	eye
MGI:109632	Rax	retina and anterior neural fold homeobox	Yes	Yes	eye, hypothalamus
MGI:97878	Rbp3	retinol binding protein 3, interstitial	Yes	Yes	eye
MGI:97883	Rcvrn	recoverin	Yes	Yes	eye
MGI:1925224	Rdh12	retinol dehydrogenase 12	Yes	Yes	eye
MGI:1929473	Rgr	retinal G protein coupled receptor	Yes	Yes	eye
MGI:97998	Rom1	rod outer segment membrane protein 1	Yes	Yes	eye
MGI:2384303	Rp1l1	retinitis pigmentosa 1 homolog (human)-like 1	Yes	Yes	eye
MGI:98001	Rpe65	retinal pigment epithelium 65	Yes	Yes	eye
MGI:1336189	Rs1	retinoschisis (X-linked, juvenile) 1 (human)	Yes	Yes	eye
MGI:2443686	Rtbdn	retbindin	Yes	Yes	eye
MGI:98227	Sag	retinal S-antigen	Yes	Yes	eye
MGI:1923203	Samd7	sterile alpha motif domain containing 7	No	-	-
MGI:2444087	Slc1a7	solute carrier family 1 (glutamate transporter), member 7	Yes	No	-
MGI:2384871	Slc24a1	solute carrier family 24 (sodium/potassium/calcium exchanger), member 1	Yes	Yes	eye
MGI:103077	Stx3	syntaxin 3	Yes	No	-
MGI:2444167	Tmem215	transmembrane protein 215	No	-	-
MGI:1330305	Trpm1	transient receptor potential cation channel, subfamily M, member 1	Yes	Yes	eye

MGI:2384781	Tspan10	tetraspanin 10	No	-	-
MGI:109571	Tulp1	tubby like protein 1	Yes	Yes	eye
MGI:88401	Vsx2	visual system homeobox 2	Yes	Yes	eye

¹Affected tissues among the 47 tissues that were considered

Table S12. Mouse genes whose predicted eye functions were supported by two of the three datasets (i.e., with a medium confidence score)

MGI ID	Gene symbol	Gene name	Mutant Strain Availability	Eye abnormality	Tissues affected by mutations ¹
MGI:1921284	4632404H12Rik	RIKEN cDNA 4632404H12 gene	No	-	-
MGI:1923144	Adal	adenosine deaminase-like	Yes	No	-
MGI:2442600	Adamts18	a disintegrin-like and metallopeptidase (reprolysin type) with thrombospondin type 1 motif, 18	Yes	Yes	eye, lung, large intestine
MGI:1927136	Arl6	ADP-ribosylation factor-like 6	Yes	Yes	adipose tissue, bone, eye, hippocampus
MGI:2387588	Best2	bestrophin 2	Yes	Yes	eye
MGI:101770	Bfsp1	beaded filament structural protein 1, in lens-CP94	Yes	Yes	eye
MGI:1859639	Cacna1f	calcium channel, voltage-dependent, alpha 1F subunit	Yes	Yes	eye
MGI:1344341	Car14	carbonic anhydrase 14	Yes	-	-
MGI:1924487	Cc2d2a	coiled-coil and C2 domain containing 2A	Yes	Yes	digits, eye, heart, kidney
MGI:1889376	Ccdc126	coiled-coil domain containing 126	No	-	-
MGI:2136343	Crb1	crumbs homolog 1 (Drosophila)	Yes	Yes	eye
MGI:2451355	Crxos	Crx opposite strand transcript 1	No	-	-
MGI:88516	Cryab	crystallin, alpha B	Yes	Yes	eye, skeletal muscle
MGI:104336	Cryba2	crystallin, beta A2	Yes	Yes	eye
MGI:104992	Crybb1	crystallin, beta B1	No	-	-
MGI:2449167	Crygn	crystallin, gamma N	Yes	-	-
MGI:2179198	Defb9	defensin beta 9	No	-	-
MGI:2141813	Dhx32	DEAH (Asp-Glu-Ala-His) box polypeptide 32	No	-	-
MGI:1354952	Dkk3	dickkopf homolog 3 (Xenopus laevis)	Yes	-	-
MGI:94926	Drd4	dopamine receptor D4	Yes	Yes	eye
MGI:95285	Edn3	endothelin 3	Yes	-	large intestine
MGI:103009	Epb4_1I2	erythrocyte protein band 4 1-like 2	Yes	-	testis
MGI:1922747	Fabp12	fatty acid binding protein 12	Yes	-	-
MGI:2444268	Fam169a	family with sequence similarity 169, member A	No	-	-
MGI:3046463	Fam19a3	family with sequence similarity 19, member A3	Yes	-	-
MGI:2685472	Frmpd2	FERM and PDZ domain containing 2	No	-	-
MGI:2443337	Fscn2	fascin homolog 2, actin-bundling protein, retinal (Strongylocentrotus purpuratus)	Yes	Yes	eye
MGI:99953	Gja8	gap junction protein, alpha 8	Yes	Yes	eye
MGI:1923993	Gje1	gap junction protein, epsilon 1	Yes	Yes	eye
MGI:95785	Gnb3	guanine nucleotide binding protein (G protein), beta 3	Yes	Yes	eye
MGI:2685519	Gpr152	G protein-coupled receptor 152	Yes	No	bone
MGI:99549	Gzmm	granzyme M (lymphocyte met-ase 1)	Yes	-	-
MGI:1926876	Impg1	interphotoreceptor matrix proteoglycan 1	No	-	-
MGI:1927642	Irx6	Iroquois related homeobox 6 (Drosophila)	Yes	Yes	eye
MGI:101776	Lhx4	LIM homeobox protein 4	Yes	-	lung, pituitary
MGI:1891259	Lrat	lecithin-retinol acyltransferase (phosphatidylcholine-retinol-O-acyltransferase)	Yes	Yes	eye, testis

MGI:2685622	Lyg2	lysozyme G-like 2	No	-	-
MGI:1333773	Mab21l1	mab-21-like 1 (<i>C. elegans</i>)	Yes	Yes	eye
MGI:96913	Mak	male germ cell-associated kinase	Yes	-	-
MGI:2150656	Man2a2	mannosidase 2, alpha 2	Yes	-	testis
MGI:1914999	Mgarp	mitochondria localized glutamic acid rich protein	No	-	-
MGI:98481	Nhlh1	nescent helix loop helix 1	Yes	No	heart
MGI:102567	Nrl	neural retina leucine zipper gene	Yes	Yes	eye
MGI:1924446	Nxnl1	nucleoredoxin-like 1	Yes	Yes	eye
MGI:1922374	Nxnl2	nucleoredoxin-like 2	Yes	Yes	eye, medial olfactory epithelium
MGI:2448607	Nyx	nyctalopin	Yes	Yes	eye
MGI:99438	Opn1sw	opsin 1 (cone pigments), short-wave-sensitive (color blindness, tritan)	Yes	Yes	eye
MGI:1888678	Otor	otoraplin	No	-	-
MGI:1916489	Pdzph1	PDZ and pleckstrin homology domains 1	No	-	-
MGI:101899	Pla2g5	phospholipase A2, group V	Yes	-	heart
MGI:3026984	Plk5	polo-like kinase 5 (<i>Drosophila</i>)	Yes	No	-
MGI:98301	Pmel	premelanosome protein	Yes	Yes	eye
MGI:1354947	Polg2	polymerase (DNA directed), gamma 2, accessory subunit	Yes	Yes	eye
MGI:2443631	Pou6f2	POU domain, class 6, transcription factor 2	Yes	-	-
MGI:1924880	Prdm8	PR domain containing 8	Yes	-	epidermis
MGI:1929459	Rabgef1	RAB guanine nucleotide exchange factor (GEF) 1	Yes	-	epidermis
MGI:2384418	Rgs9bp	regulator of G-protein signalling 9 binding protein	Yes	Yes	eye
MGI:97930	Rlbp1	retinaldehyde binding protein 1	Yes	Yes	eye
MGI:1343464	Rorb	RAR-related orphan receptor beta	Yes	Yes	eye
MGI:1097709	Rrh	retinal pigment epithelium derived rhodopsin homolog	No	-	-
MGI:1921456	Sipa1l3	signal-induced proliferation-associated 1 like 3	Yes	Yes	eye
MGI:1929519	Slc16a8	solute carrier family 16 (monocarboxylic acid transporters), member 8	Yes	Yes	eye
MGI:1351866	Slco4a1	solute carrier organic anion transporter family, member 4a1	No	-	-
MGI:892968	Tacr3	tachykinin receptor 3	Yes	-	testis, uterus
MGI:104672	Tfap2b	transcription factor AP-2 beta	Yes	Yes	digits, epidermis, kidney, lung, eye
MGI:1921597	Tldc1	TBC/LysM associated domain containing 1	No	-	-
MGI:98880	Tyr	tyrosinase	Yes	Yes	epidermis, eye, kidney
MGI:98881	Tyrp1	tyrosinase-related protein 1	Yes	Yes	bone, eye
MGI:1328357	Unc119	unc-119 homolog (<i>C. elegans</i>)	Yes	Yes	eye
MGI:1346018	Vax2	ventral anterior homeobox containing gene 2	Yes	Yes	eye
MGI:1921449	Vit	vitrin	Yes	-	-
MGI:1924662	Wdr17	WD repeat domain 17	Yes	-	-
MGI:2677168	Zfp563	zinc finger protein 563	No	-	-

¹ Affected tissues among the 47 tissues that were considered

Table S13. The number of phenotypically unannotated genes (number of genes with available mutant strain but no reported phenotypes in the 47 tissues examined; number of genes whose mutant strain has not been produced) for each set of genes with a given confidence score and a given predicted tissue function. These numbers were calculated based on the data collected in December, 2016.

Predicted tissue function	Confidence score of genes		
	High	Medium	Low
Adipose tissue	-	33 (15;18)	116 (36;80)
Adrenal gland	-	35 (13;22)	89 (21;68)
Amygdala	-	-	-
Bladder	-	-	110 (35;75)
Bone	53 (24;29)	553 (202;351)	2046 (577;1469)
Bone marrow	51 (24;27)	395 (152;243)	1832 (513;1319)
Brown fat	-	45 (21;24)	135 (37;98)
Cerebellum	82 (38;44)	572 (237;335)	1205 (338;867)
Cerebral cortex	19 (8;11)	352 (150;202)	935 (303;632)
Digits	-	-	274 (81;193)
Dorsal root ganglia	-	-	151 (52;99)
Dorsal striatum	-	-	-
Epidermis	-	73 (15;58)	282 (85;197)
Eye	21 (9; 12)	29 (12; 17)	475 (115;360)
Frontal cortex	-	-	895 (314;581)
Heart	51 (15;36)	434 (121;313)	6958 (1893;5065)
Hippocampus	21 (9;12)	382 (161;221)	1007 (330;677)
Hypothalamus	-	32 (11;21)	329 (66;263)
Kidney	-	142 (39;103)	138 (33;105)
Large intestine	4 (2;2)	83 (22;61)	516 (170;346)
Liver	-	259 (93;166)	976 (311;665)
Lung	-	53 (16;37)	403 (129;274)
Lymph node	78 (39;39)	282 (94;188)	1449 (383;1066)
Mammary gland	-	10 (2;8)	43 (10;33)
Medial olfactory epithel.	-	-	163 (45;118)
Olfactory bulb	-	9 (1;8)	414 (133;281)
Oocyte	-	1030 (176;854)	1952 (469;1483)
Ovary	-	-	35 (8;27)
Pancreas	-	-	256 (78;178)
Pituitary	-	11 (4;7)	298 (69;229)
Placenta	-	507 (135;372)	1103 (288;815)
Prostate	-	11 (4;7)	271 (46;225)
Salivary gland	-	-	-
Skeletal muscle	11 (3;8)	133 (45;88)	520 (139;381)
Small intestine	-	-	155 (51;104)
Spinal cord	-	120 (45;75)	832 (320;512)
Spleen	118 (57;61)	560 (211;349)	1746 (501;1245)
Stomach	-	23 (4;19)	67 (13;54)
Substantia nigra	-	-	-
Testis	-	1030 (176;854)	1917 (461;1456)
Thymus	34 (15;19)	167 (56;111)	1277 (336;941)
Thyroid	34 (15;19)	167 (56;111)	1277 (336;941)
Tongue	-	83 (16;67)	197 (40;157)
Trachea	-	-	274 (81;193)
Trigeminal	-	-	151 (52;99)
Uterus	-	-	64 (15;49)
Vomeronasal organ	-	-	34 (9;25)

Table S14. Candidate genes whose vision/eye phenotype have been examined by IMPC, and the gross eye morphology that have been measured in the gene deletion strains.

Gene symbol	Vision/eye phenotypes that have been examined and found to be not different between gene deletion strain and the wild type control ¹
High confidence genes	
<i>Kcnj14</i>	Retina (combined); persistence of hyaloid vascular system; retinal blood vessels pattern; retinal blood vessels structure; retinal blood vessels; optic disk; synechia; fusion between cornea and lens; lens opacity; lens; iris pigmentation; pupil light response; pupil dilation; pupil shape; pupil position; iris/pupil; corneal vascularization; corneal opacity; cornea; narrow eye opening; eyelid closure; eyelid morphology; bulging eye; eye
<i>Kcnv2</i>	Retina (combined); persistence of hyaloid vascular system; retinal blood vessels pattern; retinal blood vessels structure; retinal blood vessels; optic disk; synechia; fusion between cornea and lens; lens opacity; lens; iris pigmentation; pupil light response; pupil dilation; pupil shape; pupil position; iris/pupil; corneal vascularization; corneal opacity; cornea; narrow eye opening; eyelid closure; eyelid morphology; bulging eye
Medium confidence genes	
<i>Adal</i>	Retina (combined); persistence of hyaloid vascular system; retinal blood vessels pattern; retinal blood vessels structure; retinal blood vessels; optic disk; synechia; fusion between cornea and lens; lens opacity; lens; iris pigmentation; pupil light response; pupil dilation; pupil shape; pupil position; iris/pupil; corneal vascularization; corneal opacity; cornea; narrow eye opening; eyelid closure; eyelid morphology; bulging eye
<i>Fabp12</i>	Eye wetness; eye size; eye opacity; eye; iris pigmentation; iris/pupil light response; iris/pupil shape; iris/pupil position; iris/pupil; lens opacity; lens; corneal vascularization; corneal opacity; cornea; eyelid closure
<i>Plk5</i>	Retina (combined); vitreous; iris transillumination; corneal deposits; corneal sclerization; persistence of hyaloid vascular system; retinal blood vessels pattern; retinal blood vessels structure; retinal blood vessels; optic disk; synechia; fusion between cornea and lens; lens opacity; lens; iris pigmentation; pupil light response; pupil dilation; pupil shape; pupil position; iris/pupil; corneal vascularization; corneal opacity; cornea; narrow eye opening; eyelid closure; eyelid morphology; bulging eye; eye
<i>Wdr17</i>	Retina (combined); vitreous; iris transillumination; corneal deposits; corneal sclerization; persistence of hyaloid vascular system; retinal blood vessels pattern; retinal blood vessels structure; retinal blood vessels; optic disk; synechia; fusion between cornea and lens; lens opacity; lens; iris pigmentation; pupil light response; pupil dilation; pupil shape; pupil position; iris/pupil; corneal vascularization; corneal opacity; cornea; narrow eye opening; eyelid closure; eyelid morphology; bulging eye; eye

¹ The significance threshold of $P=10^{-4}$ by Fisher's exact test was used by IMPC

Table S15. human and zebrafish orthologs of mouse eye candidate genes

Gene Symbol	Ensembl ID	Number of human orthologs	Ensembl IDs of human orthologs	Number of zebrafish orthologs	Ensembl IDs of zebrafish orthologs (protein identity, protein similarity)
High confidence genes					
<i>Ankrd33</i>	ENSMUSG00000047034	1	ENSG00000167612	2	ENSDARG00000002508 (29.2%, 37.2%); ENSDARG00000055638 (29.0%, 40.5%)
<i>Arr3</i>	ENSMUSG00000060890	1	ENSG00000120500	2	ENSDARG00000056511 (52.5%, 67.7%); ENSDARG00000098475 (47.0%, 67.7%)
<i>Cnga1</i>	ENSMUSG00000067220	1	ENSG00000198515	2	ENSDARG00000012125 (66.1%, 73.1%); ENSDARG00000029898 (58.0%, 68.6%)
<i>Cryba4</i>	ENSMUSG00000066975	1	ENSG00000196431	1	ENSDARG00000024548 (68.4%, 80.6%)
<i>Crybb3</i>	ENSMUSG00000029352	1	ENSG00000100053	1	ENSDARG00000041301 (54.4%, 68.0%)
<i>Gm4792</i>	ENSMUSG00000053420	0			
<i>Gm9918</i>	ENSMUSG00000097050	1	ENSG00000283536	0	
<i>Grifin</i>	ENSMUSG00000036586	1	ENSG00000275572	1	ENSDARG00000075914 (47.6%, 57.0%)
<i>Kcnj14</i>	ENSMUSG00000058743	1	ENSG00000182324	1	
<i>Kcnv2</i>	ENSMUSG00000047298	1	ENSG00000168263	2	ENSDARG00000062906 (52.0%, 62.8%); ENSDARG00000076644 (55.0%, 66.2%)
<i>Lrit1</i>	ENSMUSG00000041044	1	ENSG00000148602	2	ENSDARG00000019179 (47.6%, 63.5%); ENSDARG000000099406 (46.2%, 61.0%)
<i>Lrit2</i>	ENSMUSG00000043418	1	ENSG00000204033	1	
<i>Mana</i>	ENSMUSG00000024806	1	ENSG00000120215		
<i>Pde6h</i>	ENSMUSG00000064330	1	ENSG00000139053	1	ENSDARG000000102558 (60.7%, 64.3%)
<i>Pper2</i>	ENSMUSG00000029410	1	ENSG00000156194	2	ENSDARG000000103030 (30.6%, 38.7%); ENSDARG000000104980 (47.8%, 62.3%)
<i>Ppm1n</i>	ENSMUSG00000030402	1	ENSG00000213889	2	ENSDARG00000010231 (38.1%, 53.6%); ENSDARG00000057032 (38.6%, 53.6%)
<i>Samd7</i>	ENSMUSG00000051860	1	ENSG00000187033	1	
<i>Slc1a7</i>	ENSMUSG0000008932	1	ENSG00000162383	2	ENSDARG00000060354 (25.2%, 36.6%); ENSDARG00000026248 (70.9%, 79.7%); ENSDARG00000034940 (69.1%, 79.2%)
<i>Six3</i>	ENSMUSG00000041488	1	ENSG00000166900	2	ENSDARG0000001880 (74.1%, 85.5%); ENSDARG000000051981 (54.9%, 66.3%)
<i>Tmem215</i>	ENSMUSG00000046593	1	ENSG00000188133		
<i>Tspan10</i>	ENSMUSG00000039691	1	ENSG00000182612	1	ENSDARG00000044767 (33.1%, 53%)
Medium confidence genes					
<i>4632404H2Rik</i>	ENSMUSG00000042579	0			
<i>Adal</i>	ENSMUSG00000027259	1	ENSG00000168803	0	ENSDARG00000012986 (58.3%, 68.6%)
<i>Car14</i>	ENSMUSG00000038526	1	ENSG00000118298	1	ENSDARG00000061697 (41.8%, 56.3%)
<i>Ccdc126</i>	ENSMUSG00000050786	1	ENSG00000169193	1	ENSDARG00000062695 (41.6%, 57.2%)
<i>Cxos</i>	ENSMUSG00000074365	0			
<i>Crybb1</i>	ENSMUSG00000029343	1	ENSG00000100122	1	ENSDARG00000068507 (56.9%, 68.0%)
<i>Crygn</i>	ENSMUSG00000038135	1	ENSG00000127377	2	ENSDARG00000030411 (61.2%, 75.2%); ENSDARG00000102129 (71.0%, 85.3%)
<i>Defb9</i>	ENSMUSG00000047390	0		0	

<i>Dhx32</i>	ENSMUSG00000030986	1	ENSG00000089876	2	ENSDARG00000077461 (50.2%, 66.7%); ENSDARG00000079029 (52.7%, 67.0%)
<i>Dkk3</i>	ENSMUSG00000030772	1	ENSG00000050165	2	ENSDARG00000070683 (34.7%, 46.4%); ENSDARG00000103591 (30.4%, 46.4%)
<i>Fabp12</i>	ENSMUSG00000027530	1	ENSG00000197416	3	ENSDARG0000002311 (44.0%, 60.5%); ENSDARG00000017299 (45.5%, 59.0%); ENSDARG00000099907 (34.1%, 43.2%)
<i>Fam169a</i>	ENSMUSG00000041817	1	ENSG00000198780	2	ENSDARG0000004177 (31.3%, 43.6%); ENSDARG00000059719 (25.1%, 33.7%)
<i>Fam19a3</i>	ENSMUSG00000055865	1	ENSG00000184599		
<i>Frmfpd2</i>	ENSMUSG00000108841	1	ENSG00000170324	1	ENSDARG00000074119 (24.9%, 35.5%)
<i>Gzmm</i>	ENSMUSG00000054206	1	ENSG00000197540		
<i>Impg1</i>	ENSMUSG00000032343	1	ENSG00000112706	2	ENSDARG00000074839 (24.4%, 39.0%); ENSDARG00000077187 (30.6%, 41.9%)
<i>Lyg2</i>	ENSMUSG00000061584	1	ENSG00000185674	3	ENSDARG00000056874 (36.2%, 49.8%); ENSDARG00000071701 (35.7%, 48.8%); ENSDARG00000099562 (32.9%, 47.9%)
<i>Mak</i>	ENSMUSG00000021363	1	ENSG00000111837	1	ENSDARG00000059287 (55.1%, 62.9%)
<i>Mgarp</i>	ENSMUSG00000037161	1	ENSG00000137463	0	
<i>Ofor</i>	ENSMUSG00000027416	1	ENSG00000125879	0	
<i>Pdzph1</i>	ENSMUSG00000024227	0		1	ENSDARG00000102251 (8.0%, 9.2%)
<i>Pik5</i>	ENSMUSG00000035486	1	ENSG00000185988	0	
<i>Pou6f2</i>	ENSMUSG0000009734	1	ENSG00000106536	1	ENSDARG00000086362 (66.9%, 71.9%)
<i>Rrh</i>	ENSMUSG00000028012	1	ENSG00000180245	1	ENSDARG00000039534 (58.1%, 69.1%)
<i>Slc04a1</i>	ENSMUSG00000038963	1	ENSG00000101187	1	ENSDARG00000075948 (58.0%, 68.4%)
<i>Tldc1</i>	ENSMUSG00000034105	1	ENSG00000140950	1	ENSDARG00000062951 (43.5%, 60.0%)
<i>Vit</i>	ENSMUSG00000024076	1	ENSG00000205221	1	ENSDARG00000063631 (49.7%, 60.9%)
<i>Wdr17</i>	ENSMUSG00000039375	1	ENSG00000150627	1	ENSDARG00000075098 (76.6%, 85.0%)
<i>Zfp563</i>	ENSMUSG00000067424	1	ENSG00000214189	0	

Table S16. Information of morpholino oligoes for functional validation in the zebrafish system.

Name of MO	Injected amount (ng) ³	Sequence of morpholino oligoes (length in nucleotides)	Target zebrafish gene (Ensembl ID)	Mouse ortholog of zebrafish target (confidence core)
<i>adai</i>	3	AAAGAGATCCGCTTCGGTGTCCATC (25)	ENSDARG00000012986	Adai (medium)
<i>ankrd33aa</i>	4	ACTTTAACCCCAGCCATCTGGCC (23)	ENSDARG00000055638	Ankrd33 (high)
<i>ankrd33ab</i>	4	AACTGCTGCCATCCCTAACAGATC (25)	ENSDARG0000002508	Ankrd33 (high)
<i>car14</i>	4	ACTATTCTCCCACCGCGCAACTIAC (25)	ENSDARG00000061697	Car14 (medium)
<i>ccdc126</i>	8	CTCCGCAGGAGACAGGCCAGCATG (24)	ENSDARG00000062695	Ccdc126 (medium)
<i>dhx32a</i>	3	CTGAAGAGTCACCATTCAGCCAT (25)	ENSDARG00000077461	Dhx32 (medium)
<i>dhx32b</i>	4	ATAAATCTCTTCGGTCAGTAGCTCA (25)	ENSDARG00000079029	Dhx32 (medium)
<i>dkk3a</i>	4	AGGCTGAATCCGAGCAGAACATGT (25)	ENSDARG000000103591	Dkk3 (medium)
<i>dkk3b</i>	6	TCATCGATTCAGCATCGCGTTGAG (25)	ENSDARG00000070683	Dkk3 (medium)
<i>fam169aa</i>	6	TTATTCTCTGGTGAACCTCAGTGCAT (25)	ENSDARG00000059719	Fam169a (medium)
<i>fam169ab</i>	4	GAACTCCCATCCCTAGCCCTGAGA (25)	ENSDARG0000004177	Fam169a (medium)
<i>frmpd2</i>	3	GGGTCACCAAACCGTGCCTCATCTTC (25)	ENSDARG00000074119	Frmpd2 (medium)
<i>grifin</i>	8	CTCAAACCGTAATGTCATCTCGTCT (25)	ENSDARG00000033382	Grifin (high)
<i>kcnj14</i>	3	CCATTACAGACCCCCACAGAGTGAC (25)	ENSDARG00000075914	Kcnj14 (high)
<i>lrrt2</i>	4	ACATCCATGGTCTCTATAAATGGT (25)	ENSDARG00000030626	Lrrt2 (high)
<i>pax6b</i> ¹	3	TGGTATTCTTGGAGGCATTCTGC (25)	ENSDARG00000045936	Pax6 (-)
<i>ppef2a</i>	4	GTTGATCTTCGTCATTCCATGC (25)	ENSDARG00000104980	Ppef2 (high)
<i>ppef2b</i>	4	TTGGAGCGTCCACATCCATCTC (23)	ENSDARG00000103030	Ppef2 (high)
<i>ppm1na</i>	3	CACCCCTGATCCCGGTTCAATC (23)	ENSDARG00000010231	Ppm1n (high)
<i>ppm1nb</i>	4	GCTTCTTCTAGATGTCTCATG (25)	ENSDARG00000057032	Ppm1n (high)
<i>tldc1</i>	3	CTGGAGGGAAAATCTACGATTACTTG (25)	ENSDARG00000062951	Tldc1 (medium)
<i>wdr17</i>	3	TCGCCTTACATACGCAGAGCCGAA (25)	ENSDARG00000075098	Wdr17 (medium)
<i>Standard Control</i> ²		CCTCTTACCTCAGTTACAATTATA (25)	None	-

¹Positive control

²Negative control

³Determined by the highest dosage that maintain the embryonic survival rate > 60 % at 72 hours post injection